

ZnO/MWCNT Sensors: Rejuvenation and Analysis of UV-Degassing Effects for Hydrocarbon Gases

BY

MRUDULA MANJUNATH

B.E., B N M Institute of Technology, Bengaluru, India, 2011

Affiliated to Visvesvaraya Technological University, Belgaum, India

THESIS

Submitted as partial fulfilment of the requirements
for the degree of Master of Science in Electrical and Computer Engineering
in the Graduate College of the
University of Illinois at Chicago, 2018

Chicago, Illinois

Defense Committee:

Igor Paprotny, Chair and Advisor

Michael Strocio

Alan Feinerman

ACKNOWLEDGEMENTS

First of all, I would like to thank Dr. Igor Paprotny for having trust in me and giving me this project. In Sanskrit, the word ‘Guru’ means more than just a teacher. “A Guru is the one who moulds the values, shares experiential knowledge, an exemplar in life, an inspirational source and who helps in the overall evolution of a student”. And I proudly say that Dr. Paprotny is my Guru.

He has helped me with all the resources, shared immense knowledge and supported me in completing the project on time.

I would also like to thank Dr. Michela Sainato, Alvaro Sahagun and Jiaxi Xiang for their guidance and knowledge transfer, which help me understand the project better during the initial phase of my research study.

My parents to whom I dedicate this thesis, are my greatest strength. Having a focussed mind is really important for achieving the goal. They have provided constant motivation and moral support during my hard times. Their blessings, guidance and support has made me the person I am this day.

Abhijeet Karandikar, my best friend, without whom the journey throughout the thesis wouldn’t have been easy. He was the one I turned to whenever my spirits needed a lift. I would like to heartily thank him for standing with me and supporting me.

Work for this Thesis was carried out at the University of Illinois at Chicago. All experimental work have been done by myself at Micro-mechatronic Systems Laboratory of UIC, except for the sensors fabrication, which was done at Center for Nanoscales Materials of Argonne National Laboratory by Michela Sainato.

MM

TABLE OF CONTENTS

CHAPTER		PAGE
1.	Introduction.....	1
1.1	Gas Sensors – An Overview.....	2
1.1.1	Electrochemical Sensors and Its Properties.....	3
1.2	Gas Sensing Mechanism in a Chemiresistive Sensor.....	4
1.2.1	Band Theory Behind Sensing.....	7
1.3	Materials Used for Chemiresistive Gas Sensors.....	9
1.4	Factors Influencing a Metal-oxide based Gas Sensor.....	11
1.4.1	Oxygen and Water Vapour Adsorption.....	13
1.4.2	Temperature.....	14
1.4.3	Grain Size.....	14
1.5	Carbon Nanotubes (CNTs).....	15
1.5.1	Structure of CNTs.....	17
1.5.2	Functionalization of CNTs.....	19
2.	Fabrication Technique and Experimental Setup.....	21
2.1	Atomic Layer Deposition.....	21
2.2	Fabrication Process.....	23
2.3	Experimental Setup.....	26
2.4	Experimental Process.....	28
3.	UV-Degassing Effects on ZnO/MWCNT sensors for Hydrocarbon Gases.....	31
3.1	Introduction.....	31
3.2	Photo-catalytic Properties of ZnO.....	31
3.3	Photo-catalytic oxidation of CH ₄	32
3.4	A Review on UV Photo-activation Using ZnO.....	33
3.5	Traditional Process of Measuring Sensor Response.....	35
3.6	UV – degassing Mechanism.....	38
3.7	Experimental Results.....	40
3.8	Discussion.....	44
4.	Rejuvenation of Aged Sensors.....	46
4.1	Experimental Methodology.....	46
4.2	Experimental Results and Observations.....	48
4.3	Discussion.....	50
5.	Conclusion and Future Work.....	51
5.1	Conclusion.....	51
5.2	Future Work.....	51
	Cited Literature.....	52
	VITA.....	55

LIST OF TABLES

TABLE		PAGE
I.	PROPERTIES OF HYDROCARBONS MEASURED IN THE ENVIRONMENT....	1
II.	RESISTANCE CHANGES FOR N AND P-TYPE SEMICONDUCTOR MATERIAL SUMMARY.....	9
III.	VARIOUS CHEMIRERESISTIVE MATERIALS, ADDITIVES AND ANALYSING GASES – OXIDES AND DIOXIDES.....	10
IV.	VARIOUS CHEMIRERESISTIVE MATERIALS, ADDITIVES AND ANALYSING GASES – POLYOXIDES.....	11
V.	VARIOUS PROPERTIES OF CNTs.....	17
VI.	PARAMETERS SET FOR THE UV-DEGASSING STUDY.....	37
VII.	PARAMETRS SET FOR REJUVENATION PROCESS.....	47

LIST OF FIGURES

FIGURE		PAGE
1.	Typical sensor response for a MOX based gas sensor.....	4
2.	Structure of a chemiresistive sensor.....	5
3.	Chemisorption of oxygen ions.....	6
4.	Schematics demonstrating the mechanism of an n-type Semiconducting MOX sensor's response to oxidizing and reducing gases.....	6
5.	Band theory in silicon.....	8
6.	Three classes of material according to band theory.....	8
7.	Receptor function, Transducer function and Utility factor.....	12
8.	Illustration on the generation of sensing signals upon contact with a target gas.....	13
9.	Two different mechanisms of water adsorption on SnO ₂ surface.....	14
10.	Grain size effects on SnO ₂ sensor response.....	15
11.	Types of CNTs.....	16
12.	Structures of CNTs.....	18
13.	Mechanism of a chemiresistive sensor based on CNTs.....	18
14.	Illustration of the ALD process for SiO ₂	22
15.	Illustration of uniformity, conformality and surface smoothness.....	22
16.	Fabrication processes of MOX/MWCNT sensor.....	25
17.	Fabricated sensor chips with 2 and 4 sensors respectively.....	26
18.	Setup for experiments using VOCs.....	26
19.	Setup for experiments using CH ₄	27
20.	Electrically wired sensor chip with 2 sensors.....	28
21.	Test chamber setup.....	28
22.	Data Acquisition System.....	29
23.	Gas tanks setup.....	30
24.	Photo-catalytic oxidation of methane; ZnO nanoparticles.....	32
25.	Variation in the resistance after switching on the UV-LED.....	34
26.	Resistance variation with and without UV irradiation.....	34

LIST OF FIGURES (CONTD...)

FIGURE		PAGE
27.	Sensor Response R of ZnO/MWCNT (175 ⁰ C) sensors in ohms under CH ₄ and O ₂ ...	35
28.	Sensor Response R of ZnO/MWCNT (175 ⁰ C) sensors in ohms under CH ₄ and N ₂ ...	36
29.	Histogram of relative resistance variation (ΔR) of ZnO/MWCNT (175 ⁰ C) sensors under CH ₄ with different carrier gases.....	36
30.	Schematic illustration of the photo-catalytic reaction process of CH ₄	39
31.	Sensor Response R and UV-degassing effect of ZnO/MWCNT (175 ⁰ C) sensors; Methane and O ₂ as carrier gas.....	40
32.	Sensor Response R of ZnO/MWCNT (175 ⁰ C) sensors; Toluene and N ₂ as carrier gas.....	41
33.	Sensor Response R of ZnO/MWCNT (1750C) sensors; Benzene and N ₂ as carrier gas.....	41
34.	UV-degassing effect of ZnO/MWCNT (175 ⁰ C) sensors; Methane and O ₂ as carrier gas.....	42
35.	UV-Degassing effect of ZnO/MWCNT (175 ⁰ C) sensors; Methane and N ₂ as carrier gas.....	42
36.	ZnO/MWCNT (175 ⁰ C) aged sensors initial response.....	48
37.	ZnO/MWCNT (175 ⁰ C) aged sensors response after exposure to 24 seconds of UV light.....	48
38.	ZnO/MWCNT (175 ⁰ C) aged sensors response after baking at 80 ⁰ C and then storing.....	49
39.	ZnO/MWCNT (1750C) aged sensors response after rejuvenation process.....	49

LIST OF ABBREVIATIONS

3D	Three Dimensional
ALD	Atomic Layer Deposition
CNT	Carbon Nanotube
CVD	Chemical Vapour Deposition
DAQ	Data Acquisition
GWP	Global Warming Potential
MFC	Master Flow Controller
MOX	Metal Oxide
MWCNT	Multi Walled Carbon Nanotube
PVD	Physical Vapour Deposition
SWCNT	Single Walled Carbon Nanotube
TEM	Transmission Electron Microscopy
UV	Ultra Violet
VOC	Volatile Organic Compounds

SUMMARY

In the recent decade, there has been a tremendous demand for the hydrocarbon gas sensors, in various industries as well as for home-monitoring. With the increasing incidence of industrial and household accidents and greater rise in the global warming in the recent years, it is crucial to continuously monitor the concentration of the harmful substances in the environment, hydrocarbons being the one.

The thesis discusses on the Multi-walled Carbon nanotube (MWCNT) based hetero-structure gas sensors functionalized with metal oxide (MOX) nanoparticles and their properties. UV-degassing and photo-activation of these hetero-structures are investigated for hydrocarbons detection. ZnO/MWCNT chemiresistive sensors are chosen for the study. The study focusses on obtaining faster recovery and improved sensitivity in order to achieve the baseline. The differences in UV-degassing effects on the ZnO/MWCNT structures when exposed to Methane (CH₄) and VOCs are discussed. It is observed that the UV degassing mechanism is oxygen dependent.

MOX based gas sensors are limited by their low stability over time and long range signal drift, which leads to uncertain results and the need to recalibrate or replace the sensors frequently. The gradual aging occurs due to the presence of relative humidity in the ambient room temperature conditions and also, with continuous exposure to the target gas over the time. A process to rejuvenate the aged sensors was established and the results were analysed.

CHAPTER 1

INTRODUCTION

Extensive research is going on the gas sensors because of their widespread applications in various industries. It becomes very essential to have a highly sensitive, selective and stable gas sensor for leakage detection of various explosive and poisonous gases in the industry. Also, recently, with the advancement in the gas sensing technology, they are being implemented in food industry for food control, home security, agricultural and in biomedicine fields as well.

Hydrogen and carbon atoms constitute a hydrocarbon molecule, methane being the simplest hydrocarbon molecule with one carbon atom and four hydrogen atoms attached to it. Various properties of different hydrocarbons are cited in the Table I.

TABLE I
PROPERTIES OF HYDROCARBONS MEASURED IN THE ENVIRONMENT (1)

Molecule	Molecular Weight (g/mol)	Density at 25°C (g/cm³)	Boiling temperature (°C)	Solubility in water at 25°C (g/L)
Methane (CH₄)	16	0.423	-161.5	0.0227
Benzene (C₆H₆)	78.1	0.874	80.1	1.78
Toluene (C₆H₅CH₃)	92.1	0.862	110.6	0.53
Ethylbenzene (C₆H₅CH₂CH₃)	106.2	0.863	136.2	0.161
o-Xylene [C₆H₄(CH₃)₂]	106.2	0.876	144.4	0.171
m-Xylene [C₆H₄(CH₃)₂]	106.2	0.860	139.1	0.161
p-Xylene [C₆H₄(CH₃)₂]	106.2	0.857	138.4	0.181
Naphthalene (C₁₀H₈)	128.2	1.025 ²⁰	217.9	0.0316
Anthracene (C₁₄H₁₀)	178.2	1.28	340	0.000045
Phenanthrene (C₁₄H₁₀)	178.2	1.179	340	0.0011

“The Global Warming Potential (GWP) was developed to measure the amount of energy the emissions of 1 ton of a gas will absorb over a given period of time, relative to the emissions of one ton of carbon dioxide (CO₂)” (2). The larger the GWP, larger is the given gas warming up the Earth over that time period. Methane (CH₄), the simplest hydrocarbon is estimated to have a GWP of 28–36 over 100 years. (2)

Volatile organic compounds (VOCs) like Benzene and Toluene are carcinogens. As a result, monitoring the hydrocarbons is of greater priority. Over the decade, research groups across the world have developed and conducted research on various hydrocarbon gas sensors and are still continuing experimenting on various aspects of the gas sensors.

The sensitivity, selectivity and stability are the three criteria considered for an efficient gas sensing system. However, semiconductor metal oxide suffers from a lack of selectivity of gases and needs to be operated at high temperatures. Carbon Nanotube (CNT) based sensors became a popular choice of the researchers in the recent decade due to its excellent and unique properties. But, it could detect only several strongly oxidizing gases and strongly reducing gases. As a result, metal oxides (MOXs) deposited on CNTs structures were found most promising which has the potential to solve the drawbacks of both MOX and CNT based structures.

The long-term stability of sensors is another significant parameter for the sensor's performance. This study focuses on the investigation UV-degassing effects of the MOX/MWCNT hetero-structured sensors for better sensitivity and faster recovery, and on a process to rejuvenate the aged sensors in order to achieve long term stability.

1.1 Gas Sensors – An Overview

The performance of any gas sensor is determined by the “3S” properties i.e. selectivity, sensitivity and stability. High 3S properties along with quicker recovery and room temperature operation resulting in low power consumption characterises a high performance gas sensor, which is in great demand. This demand along with the advancement in the material science field, resulted in the discovery of new sensing materials.

There are various types of sensors that are commonly used depending upon the sensing mechanism like optical sensors, piezoelectric sensors, electrochemical sensors, etc. Sensors used for the study are electrochemical in nature.

1.1.1 Electrochemical Sensors and Its Properties

Electrochemical sensors detect the changes in the electrical properties that arise due to chemical reactions on the sensor. They require specialized electrodes depending upon the sensing mechanism. Based on the principle of operation, they are classified as potentiometric, conductometric and voltammetric sensors. Conductometric sensors are further classified into resistive and capacitive sensors. A chemiresistive sensor detects the change in the resistance of the sensitive layer when it reacts with the analyte. The performance of any chemiresistive sensor is determined based on the below mentioned properties.

- a. *Selectivity*: determines the ability of the sensor to discriminate a specific gas between mixtures of gases, which is crucial in identifying target gas.
- b. *Sensitivity*: determines the ability of a sensor to detect any given concentration of the target gas, which is depicted by a slope, given as the measure of change of the measured signal per target gas concentration unit.

Sensitivity $S = R_s / R_o$, where R_s is the resistance in the presence of the target gas, R_o is the resistance of sensor in the air (baseline). Higher the value, better is the sensitivity.

It can also be represented as $S (\%) = ((R_o - R_s) / R_o) * 100$, i.e. the ratio of difference in the resistances to the resistance in the air.

- c. *Stability*: determines the ability of a sensor to provide reliable and reproducible results for a certain period of time. Accomplishment of the sensor's purpose is hampered if the sensor is not stable over a long period of time.
- d. *Response Time*: is the time required for a sensor to reach to a certain concentration value (usually 90%) from zero. A good sensor has a smaller response time.
- e. *Recovery Time*: is the time required for a sensor to return back to zero from a certain concentration value (usually 90%). In order to reuse the sensor repeatedly, the recovery time should be smaller.

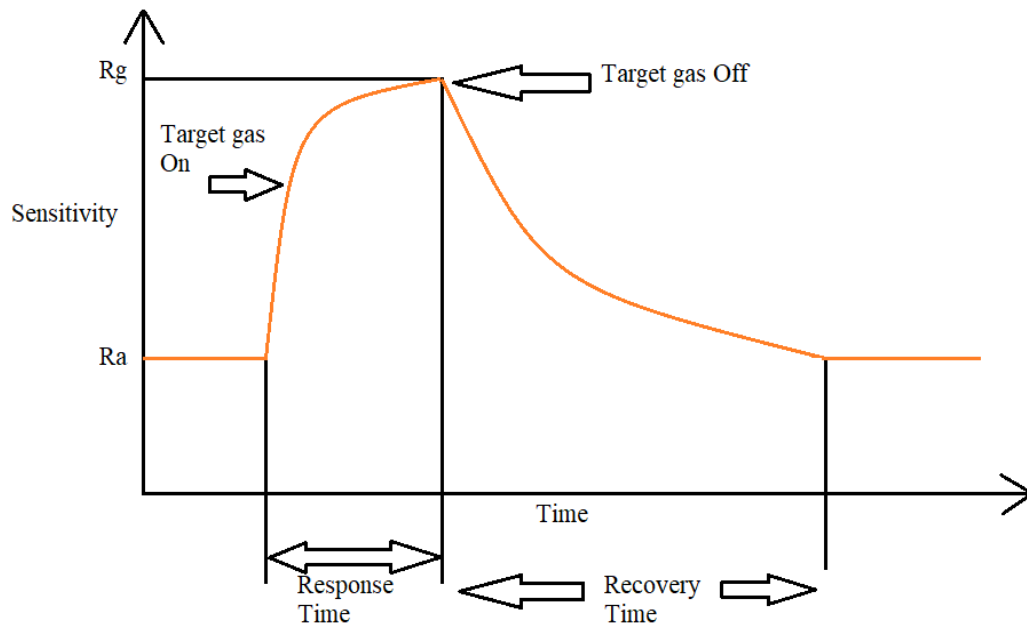


Figure 1. Typical sensor response for MOX-based gas sensor.

Most of the chemiresistive sensors use a metal oxide sensing layer, thus they are MOX-based gas sensors. The resistance change due to reaction of the metal oxide layer with the target gas is the measure of the concentration of the target gas in parts per million (ppm). Taguchi in 1962, patented the first metal oxide (Tin Dioxide, SnO_2) based gas sensor in which the electrical resistivity varies materially when exposed to inflammable gases (3). But these redox reactions requires high temperature ($>200\text{ }^\circ\text{C}$) to get activated. (4) Since, the conventional metal oxide based sensors have the drawback of poor sensitivity at room temperature, carbon nanotubes (CNTs) have caught the attention of the researchers because of their unique geometry and properties making them most favourable materials for high sensitive gas sensors which would operate at room temperature thus, resulting in low power consumption.

1.2 Gas Sensing Mechanism in a Chemiresistive Sensor

A typical chemiresistive sensor is made up of electrodes and an active sensing layer or the bulk material between electrodes, which is the selective film [Figure 2]. A change in the electrical resistance is

observed when the gas adsorption occurs on the sensing layer. This change in the resistance is measured in ohms.

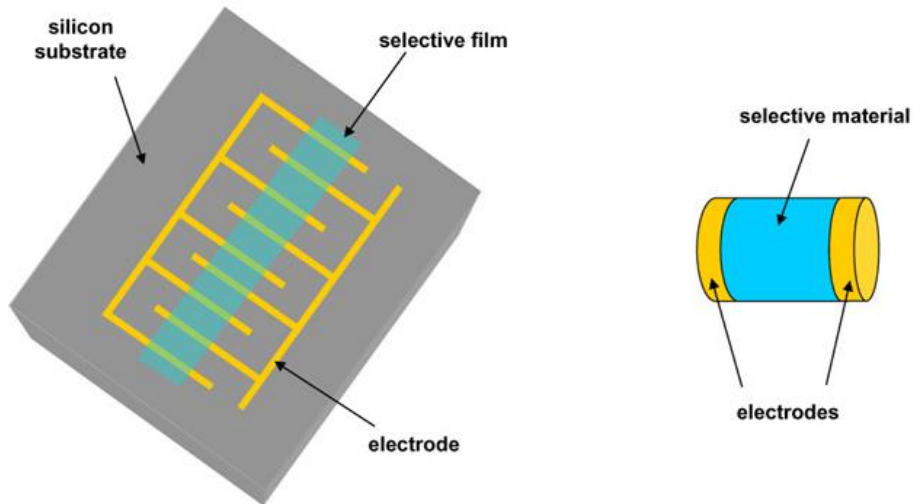


Figure 2. Structure of a chemiresistive sensor.

Basically, electron-hole pairs are generated through thermal or photo-activation and these react with the ambient oxygen or the gas surrounding the device.

An electron extraction from the conduction band occurs, forming negative sites on the surface and positive holes in the conduction band during adsorption process of oxygen molecules on the surface of the metal oxide. This results in the formation of an electron depleted region. The formation of adsorbed oxygen, either molecular or atomic depends on the temperature of the sensor [Figure 3]. With the increase in temperature, oxygen is adsorbed on the surface in the form of O^{2-} at below $175^{\circ}C$ or O^{-} ions above $175^{\circ}C$. These ions are highly reactive (5).

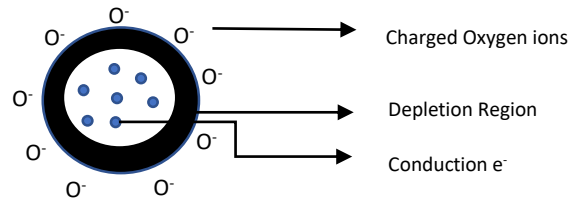


Figure 3. Chemisorption of oxygen ions.

The depletion region tends to cause an increase in the sensing film resistance after the oxygen ion adsorption. The core region of the particle where electron densities are high, has relatively low resistance. Thus, when a reducing gas is introduced, these oxygen ions react with the target gas molecules. This results in the replacement of these ions by other gas molecules thereby increasing the conductivity and decrease in resistivity. Since the oxidizing gases react with both electrons and the adsorbed oxygen ions, increases the film resistance.

Figure 4 describes the response mechanism of an n-type semiconducting MOX based sensor to oxidizing and reducing gases.

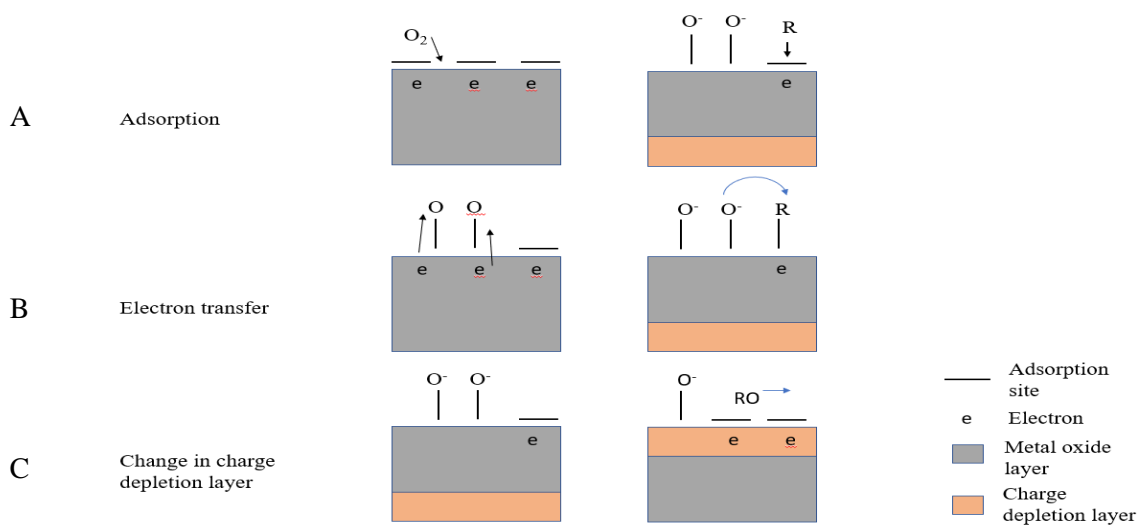


Figure 4. Schematics demonstrating the mechanism of an n-type semiconducting MOX sensor's response to oxidizing and reducing gases: A. Adsorption mechanism; B. Electron transfer mechanism; C. Change in depletion layer.

1.2.1 Band Theory Behind Sensing

The energy levels form bands when a very large number of atoms interact within the solid material. These are known as energy bands. An important parameter in the band theory is the 'Fermi level', which is the highest filled electron energy level at zero temperature. There are three types of energy bands namely, filled, valence and conduction bands. There are no free electrons available in the filled band. The lower band of an atom is the valence band. When the valence electrons gain energy, they cross across the forbidden gap and move towards conduction band. During this process, there is a flow of charges.

According to the band theory, there are three main classes of materials [Figure 6]. They are:

a. Insulator

As we know, an Insulator doesn't facilitate the flow of current. This is due to the large forbidden gap between the valence and conduction band. A very large amount of energy is necessary to shift an electron from the valence band to the conduction band. They have an energy gap of typically 10 eV and above.

b. Conductor

Conductors allow the current to flow through them easily. The absence of the forbidden gap is the reason behind the conduction, as much less energy is required to shift an electron from below the Fermi level to above the Fermi level.

c. Semiconductor

A small gap between the valence and conduction band makes semiconductor exhibit properties of both conductor and an insulator. They have an energy gap of around 0.5 – 5.0 eV. Conduction of electrons occurs when the energies are above Fermi level. (6).

For Silicon,

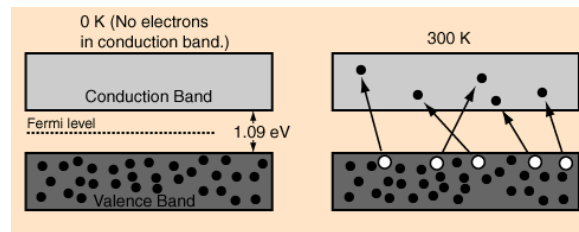


Figure 5. Band theory in Silicon (6).

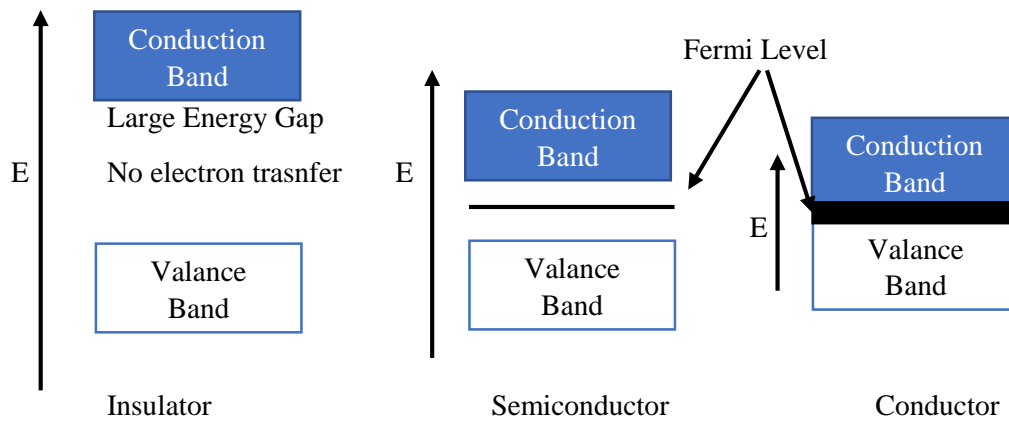


Figure 6. Three classes of material according to band theory.

A similar phenomenon occurs in the sensor's sensing material too. When the target gas interacts with the oxygen ions present on the surface of the MOX layer, a change in the charge carrier concentration occurs. Thus, a change in the resistance is observed. But, this change can be positive or negative depending on the type of the semiconductor material.

An n-type semiconductor having the electrons as their majority charge carrier, display a decrease in the resistance upon interaction with the reducing target gas. On the other hand, a p-type semiconductor with

the holes as the majority charge carrier shows an increase in the resistance. Opposite effects are seen when interacted with an oxidising gas [Table II].

TABLE II
RESISTANCE CHANGES FOR N AND P-TYPE SEMICONDUCTOR MATERIAL SUMMARY

Classification	Reducing Gas	Oxidising Gas
n-type	Decreases	Increases
p-type	Increases	Decreases

1.3 Materials Used for Chemiresistive Gas Sensors

Binary oxides like SiO₂, ZnO, TiO₂, etc. are among the most commonly used sensing layers in chemiresistive sensors.

SnO₂ is an extensively studied metal oxide for the research purpose as a result of their high sensitivity, they have an extensive demand in commercial applications (7).

Wide gap semiconductors have proven promising. Zinc oxide is II–VI semiconductor with a wide band gap of 3.37 eV (8). Doping has led to better properties of ZnO. This is the reason for its demand as a sensing material for the chemiresistive gas sensors. Added to the above properties, their high mechanical and chemical stability, low cost and lower crystalline temperature have resulted in their high sensitivity to various gases. The microstructural features such as the grain size, geometry and connectivity influences the sensitivity of ZnO materials. (9)

Tin oxide is one of the various semiconductors which has proven its high sensitivity towards various gases, but is limited by low selectivity. (10)

Titanium dioxide is popular because of its lower cross-sensitivity to humidity than other metal oxides. They also exhibit high selectivity. (10)

Tables III and IV gives an assessment on the various metal oxides, its additives and the analysing gases that are being employed by chemiresistive sensors.

TABLE III
 VARIOUS CHEMIRERESISTIVE MATERIALS, ADDITIVES AND ANALYSING GASES (11)
 OXIDES AND DIOXIDES

Chemiresistive Material	Base Material	Additives	Analysing Gas
Metal Oxides	ZnO	Al, Sn, Cu, Pd, Fe ₂ O ₃	Ammonia, Hydrogen, LPG, Methane, Carbon monoxide, Hydrogen Sulphide, Nitrogen dioxide, Methanol, Propyl Alcohol, Ethanol
	CuO	SnO ₂	Carbon monoxide, Ethanol, Hydrogen sulphide
	NiO	Li, TiO ₂	Hydrogen, Formaldehyde, Methane, Acetic Acid, Carbon Monoxide, Nitrogen dioxide
	SnO ₂	Pt, Ag, Pd, Os, Fe, Au, In, Ru, Bi ₂ O ₃ , CeO ₂ , CuO	Carbon monoxide, Methane, Sulphur dioxide, Nitrous Oxide, Carbon dioxide, Nitrogen dioxide, Propane, Methanol, Ethanol, Hydrogen, LPG, Hydrogen sulphide, Ammonia, C _n H _{2n+2} , Toluene
	TiO ₂	La, Pt, Cr ₂ O ₃ , WO ₃	Methanol, Ethanol, Propyl Alcohol, Nitrogen dioxide, Oxygen, Hydrogen, Ammonia
	CeO ₂	SnO ₂	Oxygen, Hydrogen, Sulphide

TABLE IV
POLYOXIDES (11)

Chemiresistive Material	Base Material	Additives	Analysing gas
Metal-Oxides	Al ₂ O ₃	Al, SiO ₂ /Si	Humidity, Methane, Ammonia
	Sb ₂ O ₃	Sb ₂ O ₃	Smoke, Carbon monoxide, Nitric Oxide
	Cr ₂ O ₃	TiO ₂	Nitrogen Oxide, Oxygen, Ammonia, Humidity
	Co ₃ O ₄	SiO ₂	Ammonia, Carbon Monoxide, Methane, Propane, Hydrogen, Nitrogen dioxide, Chlorine
	Fe ₂ O ₃	Au, Zn, (Pt, Pd, RuO ₂)	Methane, Propane, Benzene, Toluene, Carbon monoxide, Nitrogen dioxide, Methanol, Acetone
	Ga ₂ O ₃	SnO ₂ , Pd, Ta ₂ O ₅ , WO ₃ , NiO	Oxygen, Carbon monoxide, methane, nitric oxide, ammonia
	In ₂ O ₃	MoO ₃ , Au, Al, SnO ₂	Ozone, Nitrogen dioxide, Hydrogen, Carbon monoxide, Propane, Hydrogen Sulphide, Chlorine, Carbon dioxide, Sulphur dioxide, Ammonia, Ethanol, Acetone
	MoO ₃	Ti	Ammonia, Carbon monoxide, Nitrogen dioxide
	Nb ₂ O ₅	SnO ₂	Ammonia, Carbon monoxide, Ethanol, Hydrogen
	WO ₃	Mg, Zn, Mo, Re, Au, Pd	Nitrogen dioxide, Ammonia, Hydrogen sulphide, Ozone
	V ₂ O ₅	Fe ₂ O ₃ , SnO ₂ , TiO ₂	Nitrogen dioxide, Ammonia, Ethanol, Butyl amines, Propanol, Toluene

1.4 Factors Influencing a Metal-oxide based Gas Sensor

Three main factors that influence sensing performance of a MOX based gas sensors are receptor function, transducer function and utility factor [Figure 7] (12).

a. Receptor Function

Refers to the ability to interact with the target gas by the oxide surface. Addition of an additive such as noble metals, acidic or basic oxides on the metal oxide surface modifies the receptor function to achieve a better sensitivity.

b. Transducer Function

Conversion ability of the sensors from signal generated by chemical reactions taking place on the metal-oxide surface to an electrical signal is determined by Transducer function. This function is exhibited by each boundary between grains using a double-schottky barrier model.

The inferred barrier height and the concentration of the target gas plays an important role in the resistance changes.

c. Utility Factor

Expresses the accessibility of inner oxide grains to the target gas. Grains present at inner sites are not accessible by the target gas molecules if the rate of the target gas reaction is greater than that of gas diffusion. This results in the loss of gas response.

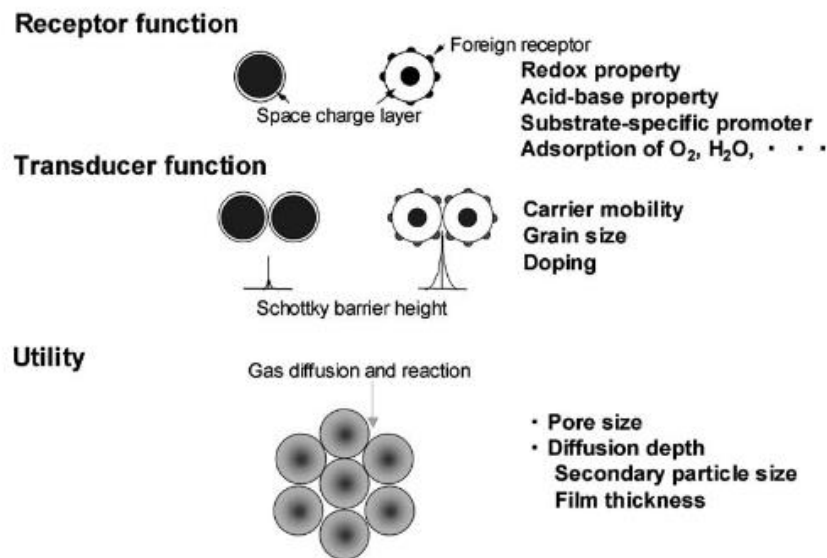


Figure 7. Receptor function, Transducer function and Utility factor (12).

Figure 8 shows an illustration of the sensing signals generation by a semiconductor material when exposed to a target gas. Surface of each particle of a semiconductor provides the receptor function due to chemical reaction which is then transduced through the microstructure of coagulating particles into polycrystalline element's resistance, generating an output resistance change (13).

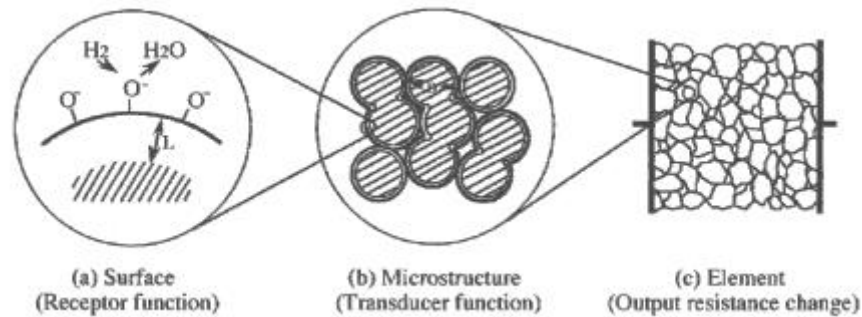


Figure 8. Illustration on the generation of sensing signals upon contact with a target gas (13).

Some of the other factors that influence the performance of the MOX based sensors as discussed below.

1.4.1 Oxygen and Water Vapor Adsorption

Oxygen is adsorbed in the form of O^{2-} or O^- on the surface of the sensing material. Desorption of the oxygen ions or their reaction with the surrounding target gas will cause decrease in the resistance and in turn increase in the conductance of the sensing material. Depending on whether the target gas is a reducing gas or an oxidising gas, the sensing mechanism differs, which is as discussed before in section 1.2.

Water vapor adsorption also plays an important role on the performance of the sensor. It has been observed that the interaction of water and the surface is strongly dependent on the operating temperature (14).

Two main mechanisms briefly summarizes the adsorption process as shown in the example Figures A and B [Figure 9] for water adsorption on SnO_2 surface. Two hydroxyl groups are generated in the first mechanism, one from the water molecule dissociation and the other from the reaction between hydrogen and oxygen in the metal oxide structure. Water molecules react with adsorbed oxygen ions to form hydroxyl groups and release an electron to the conduction band, in the second mechanism (15).

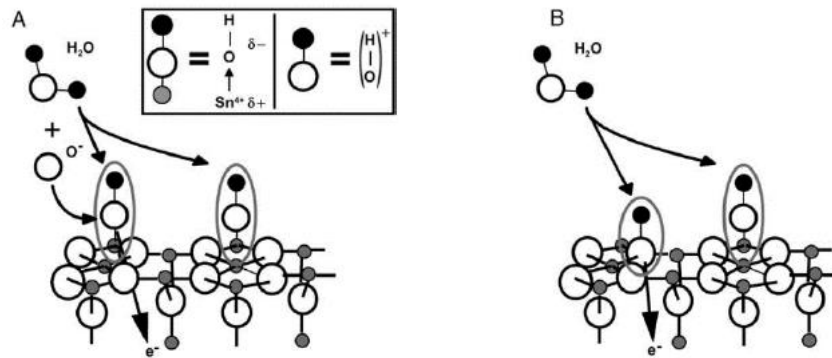


Figure 9. Two different mechanisms of water adsorption on SnO₂ surface (15).

The hollow structure of MWCNT and the surface defects has enabled it to be used as humidity sensing material. L Liu et al. observed that the resistance of MWCNTs increases linearly with increasing the relative humidity from 25% to 95% RH (16).

1.4.2 Temperature

Temperature is another important parameter that affects the gas sensing properties. Sensitivity and the response time of the sensors is significantly affected by the variation in the operating temperature. The thermionic transmission due to increase in the temperature results in the decrease in the resistance as the electrons move away from the surface. As a result, chemiresistive sensors display better sensitivity at higher operating temperatures (>200°C), the drawback of it is high power consumption.

1.4.3 Grain Size

Dimension of the nanostructure influences the sensor's sensitivity. Dimension of the nanostructure if twice the Debye length, results in a good sensitivity of the material (17).

Debye length is the distance over which significant charge separation can occur when depletion region is created. The grain size can neither be very large nor very small. Insufficient amount of electrons due to very smaller grain size, will hamper the sensor's stability. And, very large grain size of the nanomaterial does not affect the sensing response significantly.

Figure 10 shows the influence of grain size on sensor response in SnO₂ sensors at 300°C.

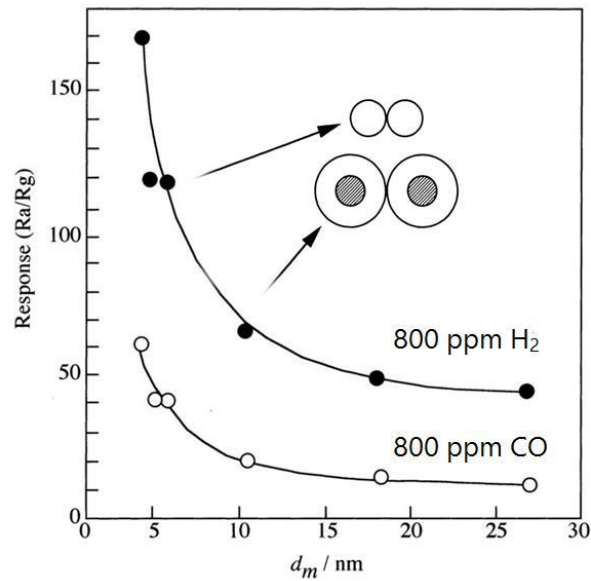


Figure 10. Grain size effects on SnO₂ sensor response (13).

1.5 Carbon Nanotubes (CNTs)

CNTs are basically allotropes of carbon with a cylindrical nanostructure. The very first fullerene-related carbon nanotubes were discovered by Sumio Iijima in 1991. Based on their structure, they are of two types namely, Single walled CNTs (SWCNT) and Multi-walled CNTs (MWCNT) [Figure 11].

A SWCNT is made up of a single atom thick layer of graphite rolled up into a cylinder with a diameter ranging from 0.4 nm to 6 nm and length between one to hundred microns (18). MWCNTs are made up of multiple layers of graphene bundled together to form a concentric cylinders because of the strong interaction between CNT's, all of which sharing the same central axis. Their diameter ranges to several nanometers.

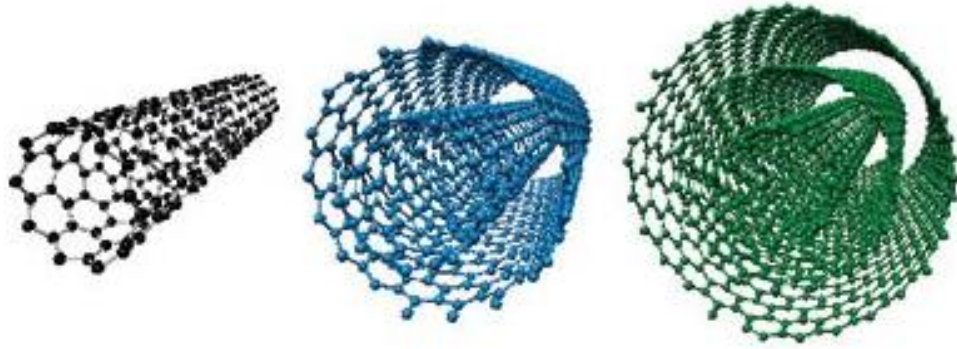


Figure 11. Types of CNTs (19).

Due to its cylindrical structure, CNTs have a larger aspect ratio (width vs. length). This property of a CNT enables the carbon atoms to easily interact with the surrounding gas molecules and detect even a lower concentration of the gas. In addition, they have the ability to operate at room temperature and exhibit quick response due to their electrical properties. This leads to the low power consumption, which is a very big plus factor. Their high sensitivity and easy miniaturization provides an added advantage over the conventional metal-oxide based sensors.

Various properties of the CNTs are summarized in the Table V below (20).

TABLE V
VARIOUS PROPERTIES OF CNTs (20)

Property	Carbon Nanotubes
Lattice structure	(Cylindrical) hexagonal lattice helicity Nanotubes: ropes, tubes arranged in triangular lattice with lattice parameters of $a = 1.7\text{nm}$, tube-tube distance = 0.314
Specific gravity	0.8-1.8 gcc^{-1}
Elastic modulus	~1 TPa for SWNT ~0.3-1 TPa for MWNT
Strength	50-500 GPa for SWNT 10-50 GPa for MWNT
Resistivity	~5-50 micro-ohm cm
Thermal Conductivity	3000 $\text{W m}^{-1}\text{K}^{-1}$ (theoretical)
Thermal expansion	Negligible (theoretical)
Oxidation in air	>700

1.5.1 Structure of CNTs

The chiral index basically defines the direction in which the graphene sheet is rolled up, commonly known as chirality. It is denoted as (n_1, n_2) . Based on the chiral indices (n_1, n_2) , CNTs can be classified as zigzag and armchair structures. n_1 and n_2 values are equal for armchair CNTs, whereas n_1 or $n_2 = 0$ for zigzag structure. CNTs with other indices values are considered to have chiral structure [Figure 12]. They exhibit metallic or semiconducting properties based on the structure.

The sp^2 bonds in graphene are stronger as compared to sp^3 bonds in diamond. This property of graphene makes it the strongest material (21).

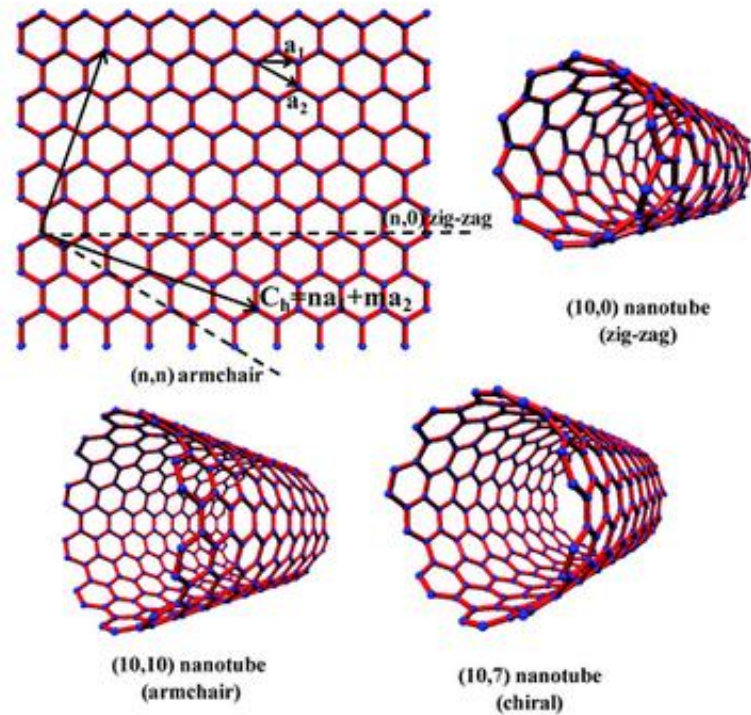


Figure 12. Structures of CNTs (22).

A functionalized chemiresistive sensor is shown in the Figure 13 below. The nanotubes act as the conducting channel between the electrodes. Sensitivity is determined by measuring the conductance changes between these electrodes. The working mechanism of the CNT based sensor is similar to as explained in section 1.2.1.

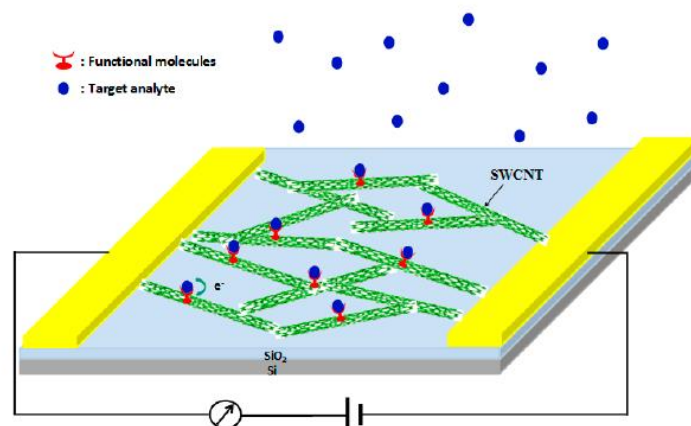


Figure 13. Mechanism of a chemiresistive sensor based on CNTs (23).

1.5.2 Functionalization of CNTs

The types of gases that can be adsorbed by pristine CNT are limited. A few strongly oxidizing gases and strongly reducing gases such as oxygen (O₂), nitrogen-dioxide (NO₂), ammonia (NH₃), and sulphur dioxide (SO₂) can be very well detected by pristine CNT. This is due to the weak interaction between the nanotubes and the target analyte molecules. As a result, functionalization of CNTs are necessary in order to improve sensitivity and selectivity of these CNT based chemiresistive sensors (24).

There are two kinds of functionalization:

1. *Covalent Functionalization:*

With this kind of functionalization, the small organic molecules, polymers or metal nanoparticles are covalently linked on the surface of the CNTs. It can be performed at the end caps of nanotubes or at their sidewalls where numerous defects are present (25). A change of hybridization from sp² to sp³ is performed during direct covalent sidewall functionalization, which involves reaction with molecules of a high chemical reactivity such as free radicals, carbenes and diazonium ions.

There are two major drawbacks with covalent functionalization:

- i. A change of hybridization from sp² to sp³ results in severe degradation in mechanical properties of CNTs.
- ii. Strong oxidants or concentrated acids often used are environmentally unfriendly.

2. *Non- Covalent Functionalization:*

The non-covalent functionalization is performed by wrapping and adsorptive forces like π - π stacking interactions or hydrophobic interaction. It is advantageous in a way that it doesn't destroy the CNT's sidewalls, and thus, the final structural properties stay intact. This is an alternative method for tuning the interfacial properties of nanotubes (25).

MWCNT functionalized with MOX nanoparticles is used in this work. The metal oxide nanoparticles are employed as photo catalysts, which can absorb light and accelerate the reaction on the film surface without any change after each cycle of reaction. Most of the semiconductor photo-catalysts are n-type semiconductor materials, including TiO₂, ZnO, SnO₂ and CeO₂. The main advantage of this kind of sensors

are its room temperature operation. This is because, the energy required for the reactions are obtained from photon (photo-activated) rather than the heat (thermally activated) from high operating temperature.

In case of photo-catalysts, the diffusion rate is thousands of times when the gas comes in the affinity of the carbon nanotubes, than when the target gas passes through the conventional catalyst particles (26).

Zinc Oxide (ZnO) was employed as the photo-catalyst in our work which was deposited through

Atomic Layer Deposition as discussed in the next chapter.

CHAPTER 2

FABRICATION TECHNIQUE AND EXPERIMENTAL SETUP

In general, metal-oxide and CNT composite materials can be classified as *metal-oxide decorated CNTs* and *CNT doped metal-oxide*. This classification is done based on the material constituting greater percentage of the composition.

1. *Metal-oxide decorated CNT*: Functionalization of the CNTs is performed during which the metal-oxide particles are attached onto the side walls of the nanotubes. This enhances the properties of the CNTs and has resulted in its extended applicability in various industries. Specially, in gas sensing applications, they have proven an improved sensitivity, faster response and recovery times and room temperature operation. The work presented in this thesis uses a chemiresistive hydrocarbon sensor fabricates using metal-oxide decorated MWCNTs.
2. *CNT doped metal-oxide*: CNTs are embedded within the metal-oxide matrix.

The sensors used for this work have the surface of the MWCNTs that were pre-treated using oxygen plasma and then the MOX nanoparticles were deposited on the surface between the gold electrodes using ALD process. This study mainly concentrates on the ZnO based MWCNT sensors.

2.1 Atomic Layer Deposition

Atomic layer deposition (ALD) is a vapour phase technique similar to chemical vapour deposition (CVD), used to deposit thin films onto the substrate during chip making. The substrate surface is exposed to alternating precursors, which do not overlap but introduced sequentially. A wide range of materials can be deposited using ALD including oxides, metals, sulphides, nitrides and fluorides.

In ALD unlike CVD process, the deposition process is split into half-reactions, each of are well-controlled.

Figure 14 shows an illustration of the ALD process for SiO₂.

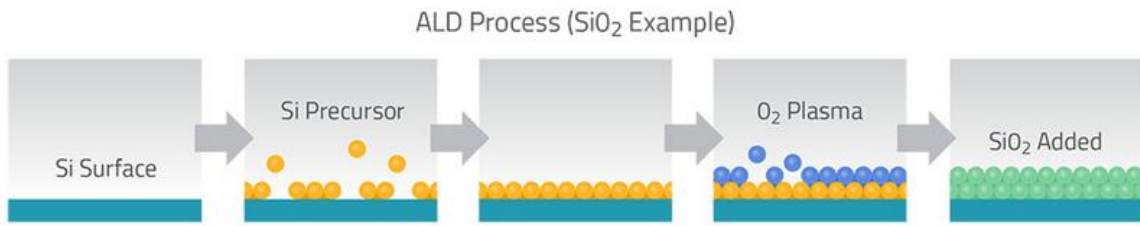


Figure 14. Illustration of the ALD process for SiO_2 (27).

Advantages:

1. Excellent uniformity is achieved all over the wafer. ALD creates an identical film thicknesses deposited on all the sides of the device (27).
2. Conformal coating can be achieved even in high aspect ratio and complex 3D structures.
3. The surfaces are atomically smooth, with uniform chemical composition.

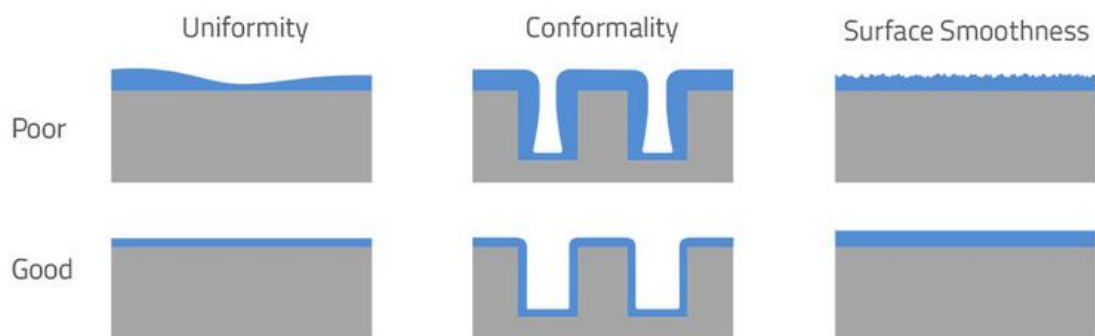


Figure 15. Illustration of uniformity, conformality and surface smoothness (27).

2.2 Fabrication Process

The fabrication process of the sensors used for the study is given in various steps below (28).

Step 1: Cleaning and drying of the wafer

A 4" quartz wafer is pre-treated by Hexamethyldisilazane (HMDS) is put into the isopropyl solution. The silicon wafers are cleaned using ultrasonic technology using acoustic energy in the ultrasonic frequency range. The ultrasonic source produces a longitudinal wave with vibrational energy due to its oscillations, which eventually propagates through the fluid. Next, the wafer is dried using N₂. The hydroxyl group formed will affect the adhesion between photoresist and substrate. Thus, the wafer is heated in the oven at 150°C for 25 minutes in order to remove the hydroxyl group.

Step 2: Coating

The wafer is cooled down and spin coating is performed on it. Spin coating process involves four steps. In the deposition stage, the coating material is applied on top of the substrate. Liquid's viscosity and the substrate's size is taken into account. In the next stage, due to the centrifugal force, the liquid spreads uniformly over the substrate. A bilayer of microchem lift-off resists 3A (LOR 3A) and S1813 photo resists were spin-coated on the wafer. Spin speed was set to 3000 rpm for 35 seconds. The coated substrate is then spun at a higher speed so that the excess liquid flows outwards and drop outside the perimeter. Evaporation of the solvent from the substrate using hotplate at 115°C for a minute is performed in the final stage. This results in an increase in the density of the photo resist. It is important to make sure the alignment of the mask is perfect. The mask is then exposed to a direct laser writer (LW 405) [Figure 16 B].

Step 3: Photoresist Development

To remove the exposed pattern on the photo resist, the wafer was soaked in the developing solvent (MF 315 and water mixed at ratio 3:1) for 30-35 seconds. After developing, wafer is then cleaned in dionized water (DI) and dried in a jet of nitrogen gas [Figure 16 C].

Step 4: Au/Cr metal deposition

After the development process of the Si wafer, a 100nm Au film on top of a 10nm Cr layer is deposited on the patterned photoresist using PVD 250 Lesker e-beam evaporator [Figure 16 D].

Step 5: Photoresist removal

Deposited metal was ‘lifted off’ by ultrasonically the samples immersed in an 1165 remover bath. The gaps between the electrodes ranged from 5 μm to 10 μm [Figure 16 E].

Step 6: CNTs deposition

Sigma Aldrich supplies a batch of 98% pure MWCNT with 12 nm average diameter, 10 μm average lengths, and a specific surface area of $\sim 220 \text{ m}^2/\text{g}$. The wafer was dosed to chips with 2 or 4 sensors on each and then baked at 75°C . An ultrasonicated solution of 1 mg/ 50 mL of MWCNT/ethanol was used to produce well dispersed CNT mesh between the electrodes. 50 μL of aliquot was deposited on a 1 mm^2 active area of the fabricated metal electrodes using micro-syringe. Baking helped in the removal of the solvent and to improve adhesion between MWCNT and the substrate [Figure 16 F].

Step 7: O₂ plasma / UV-O₃ treatment

The chips were treated by O₂ plasma for 10 seconds inside a reactive ion-etching chamber (March RIE) and a UV-O₃ chamber (Nanomax Ultra- 100) for duration varying from 5 to 60 minutes, to prepare the surface before ZnO deposition by ALD process. Plasma is used to lower the deposition temperature. Quality of the film and high deposition rates are maintained [Figure 16 G].

Step 8: Atomic Layer Deposition (ALD)

Diethylzinc (DEZ) ((C₂H₅)₂Zn) was employed as a precursor of ZnO nanoparticle deposition. ALD was performed at various temperatures ranging from 175 to 225 $^\circ\text{C}$. The deposition process consists of 48 cycles, in order to obtain the thickness of around 7.74 nm – 10.8 nm on the MWCNT surface, which was confirmed by transmission electron microscopy (TEM) [Figure 16 H].

The electrical conductivity of the fabricated electrodes, the CNT-deposited resistive network and ALD functionalized MWCNTs devices were measured using a digital multimeter. The resistance of the chemiresistor ranged between 100 Ω to 5 M Ω .

VEGA 3 (Tescan) scanning electron microscope (SEM) was then used to characterize the ZnO functionalized MWCNTs. It was also used to perform the Energy-dispersive X-ray spectroscopy (EDX) on the ZnO/MWCNT chips.

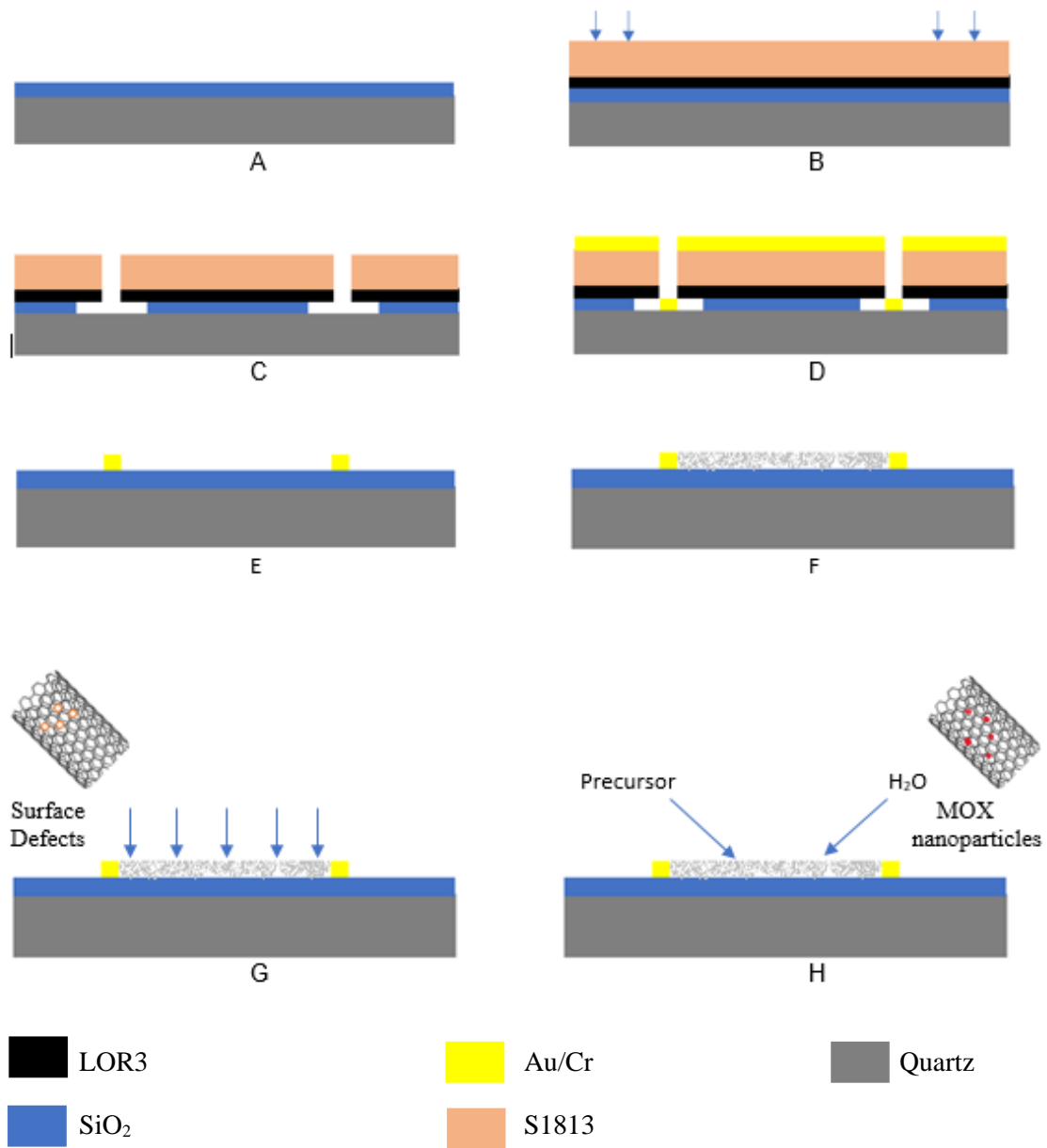


Figure 16. Fabrication processes of MOX/MWCNT sensor: A. Cleaned quartz wafer; B. Photo-resist coating and laser writing; C. Development; D. Au/Cr metal deposition; E. Photo-resist removal; F. MWCNT deposition; G. O₂ plasma treatment; H. ALD deposition.

The fabricated and diced chip with sensors are shown in the Figure 17.

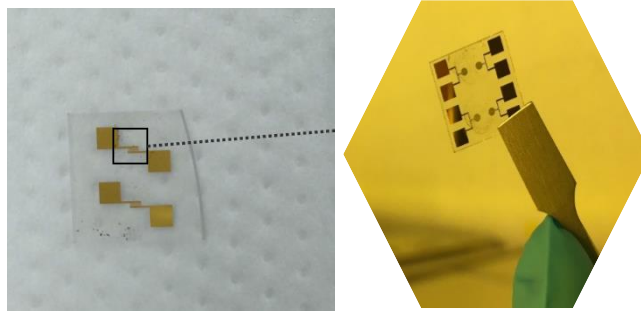


Figure 17. Fabricated sensor chips with 2 and 4 sensors respectively.

2.3 Experimental Setup

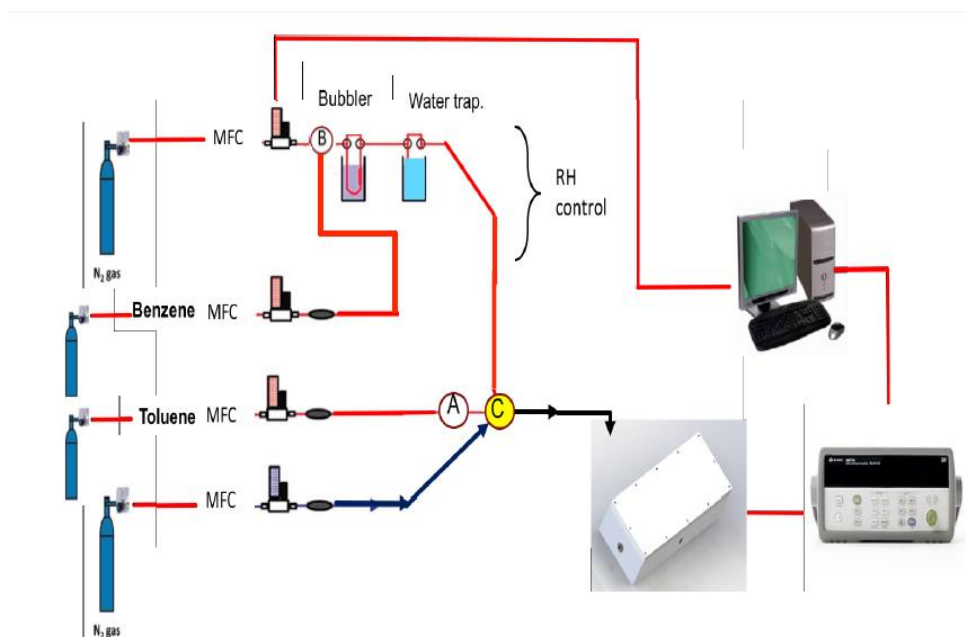


Figure 18. Setup for experiments using VOCs.

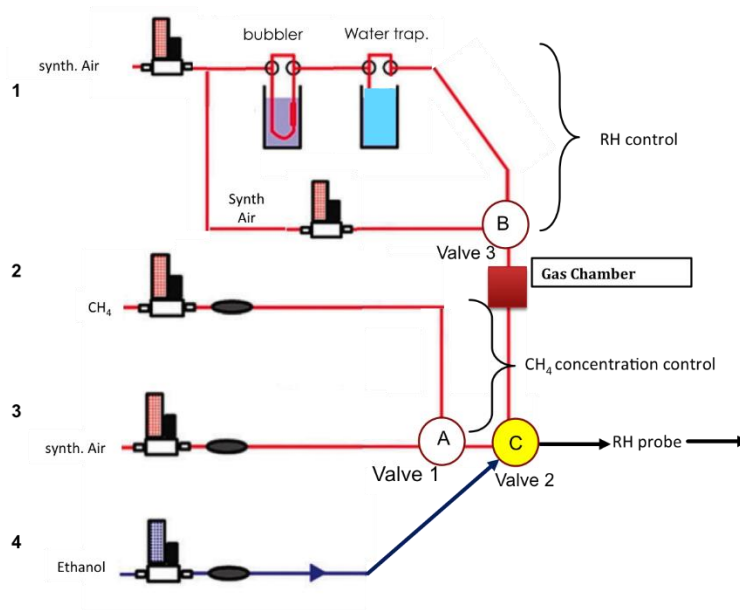


Figure 19. Setup for experiments using CH₄.

Wires are soldered onto the sensor electrodes for the convenience of connecting to the DAQ (Data Acquisition system) for the experimental purpose. The MOX/MWCNT sensors are placed in a sealed test chamber made of Teflon, covered by a plexi glass. The wires that act as the sensor electrodes have been connected to a DAQ (34972A LXI, Keysight, Inc.) which is pre-connected to a DC power supply (Model 1693, BK Precision).

Dry N₂ and synthetic air (20.8% O₂, N₂ balance) are used as carrier gas for VOCs (Toluene and Benzene) and CH₄ respectively. These are known as ‘carrier gases’, which help in purging the target gas from test chamber after each cycle of the sensor’s exposure to the target gas. They also help in removing humidity within the chamber.

Carrier gas is introduced to the test chamber at a constant flow rate of 2 SLPM (Standard Litre per Minute), which is controlled by the Mass Flow Controller (MFC). The raw data i.e. the resistance values acquired from the sensors are transferred from the DAQ to the PC which is being programmed using Labview.

2.4 Experimental Process

1. Soldering and electrical connections

The wires are soldered onto the electrodes of the sensors as shown below [Figure 20]. These wires act as the electrodes through which the voltage is given to the sensor.

The sensors are placed in the Teflon test chamber [Figure 21], sealed with the plexi glass. The wires are connected to the data acquisition (34972A LXI, Keysight, Inc.) [Figure 22] pre-connected to a DC power supply (Model 1693, BK Precision). The Resistances of sensors are read from the data acquisition system.

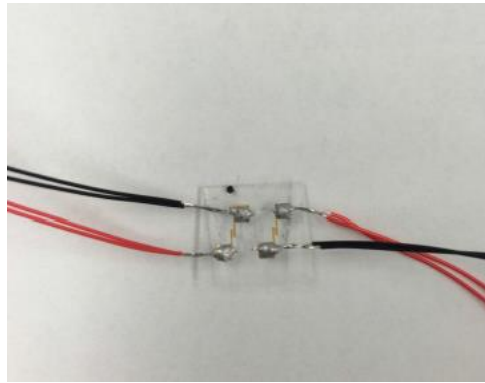


Figure 20. Electrically wired sensor chip with 2 sensors.

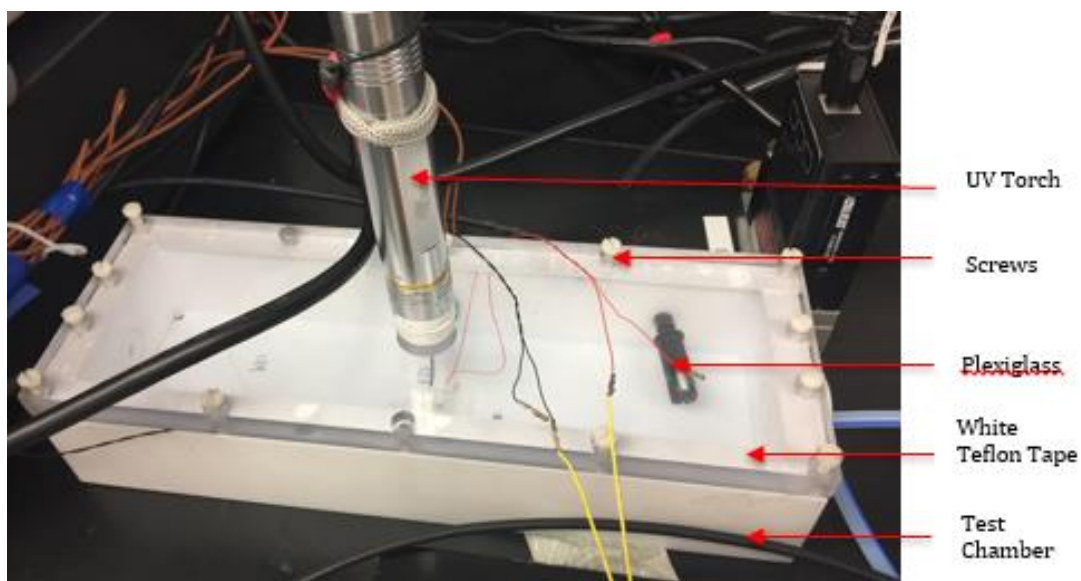


Figure 21. Test chamber setup.

There is a lining of Teflon tape under the Plexiglass and the upper surface of the chamber in order to avoid the gas leakage.



Figure 22. Data Acquisition System.

Data acquisition (DAQ) samples the measured analog signal and converts them into digital values that is understandable by a computer. On clicking the 'Mon' button, the initial resistance values of each of the sensors connected to the respective channels can be viewed.

2. Open the carrier gas and target gas tanks

The carrier and target gas tanks are opened appropriately as per the requirement of the experiment.

CHAPTER 3

UV-DEGASSING EFFECTS ON ZNO/MWCNT SENSORS FOR HYDROCARBON GASES

3.1 Introduction

In general, researches have been done on two types of activation that is being employed to trigger the operation of the MOX based gas sensors. They can be activated by using either heat or by UV light.

One major drawback using thermal activated sensors are that they cannot be used to detect flammable and explosive gases. This limitation can be eliminated by implementing UV illumination to photo-activating the sensors. Saura in 1994 first developed an UV activated SnO₂ pyrolytic films to detect trichloroethylene and acetone vapour at room temperature. The main idea of irradiating UV on the surface of the sensor film is that it changes its resistance. This is due to the generation of electron-hole pairs required for gas sensing. With the photo-excitation, the density of charge carriers increases throughout the material (29) (30). Some of the advantages of UV photo-activation that have been observed are:

- Improved sensitivity
- Quicker recovery and response time
- Long term stability
- Avoid long range signal drift
- Achieve selectivity with different intensities of UV

3.2 Photo-catalytic Properties of ZnO

The word photo-catalysis includes two words, 'photo' and 'catalysis'. Modification in the rate of a chemical reaction without altering the reactants is known as *Catalysis*. And the substance that increases the reaction rate is a Catalyst. This process results in the reduction in the activation energy. In photo-catalysis, light plays the role of activating a catalyst. A photo-catalyst modifies the rate of a chemical reaction upon light irradiation. (31)

Semiconductor oxides such as ZnO, TiO₂, SnO₂ and ZrO₂ have been found to be attractive photo-catalysts. ZnO is considered to be the most preferred photo-catalyst. This is because of its band gap of 3.2 eV with a relatively large quantum efficiency (32). "Quantum efficiency (QE) is the measure of the effectiveness to produce electronic charges from the incident photons". This property along with its unique electrical

properties, ZnO is widely being used in Sensor technology (33). High optical activity, photo-chemical stability and high surface energy are some of the other properties that support photo-catalytic nature of ZnO.

Having free exciton binding energy as large as 60 meV at room temperature, ZnO supports an efficient excitonic emission. Also, it has a band gap that corresponds to the UV region (34). It is essential to irradiate ZnO with a light with energy equal to or higher than its band gap. This results in the generation of electron-hole pairs, which then participates in the photo-catalytic process. Due to this reason, a UV light of intensity 365nm (3.3968 eV) is used for this study purpose.

3.3 Photo-catalytic Oxidation of CH₄

It has been observed that the sensing of Methane is a photo-catalytic process. ZnO being photo-catalytic in nature, when exposed to visible light, surface electrons e⁻ along with oxygen ions O⁻ and zinc radicles Zn[•] are created. Factors such as surface additives, temperature and humidity affects the surface as discussed earlier and in turn the photo-catalytic activity of ZnO (35). In order to regain long term stability and avoid long range signal drift, a possible mechanism has been proposed using UV in order to re-establish the electrical and photo-catalytic properties based on re-excitation. UV light of wavelength 365nm is irradiated on to the ZnO surface (i.e. Zn²⁺ centers) in order to re-establish the formation of Zn[•]. Thus, the sensitivity towards CH₄ is regained. Upon UV illumination, the photo-activated O⁻ ions that are induced on the ZnO surface reacts with the target gas molecules. Zinc radicals (Zn[•]) may play an important role in CH₄ detection as photo-catalysts.

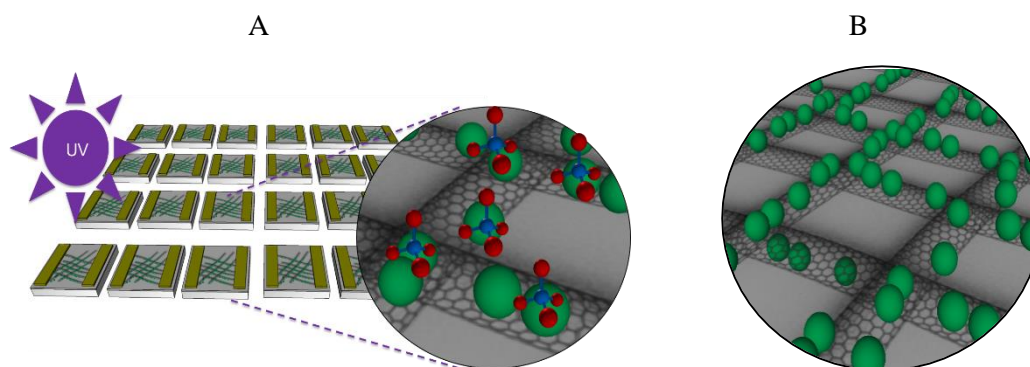
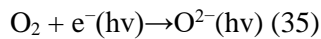
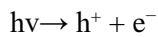


Figure 24. A. Photo-catalytic oxidation of methane; B. ZnO nanoparticles.

3.4 A Review on UV Photo-activation Using ZnO

Previously, studies have been performed on UV photo-activation using ZnO in order to achieve improved sensitivity, quicker recovery and response time and long term stability of the sensors. Photo-response behaviour of ZnO was first observed by Mellow in 1954. According to the studies, gaining stability of the sensors over a long time is still a perplexing issue and researchers are working on to find an effective solution to avoid long range signal drift due to the long term instability. At a high temperature, diffusion and sintering effects at maximum grain boundaries are possible factors for long range drift issue (36). UV irradiation is a technique that could possibly solve this issue.

UV light is irradiated throughout the gas sensing process. The target gas considered for the study by the author was H₂. Upon UV irradiation, electrons are generated in large number which causes a reduction in the depletion layer width. This procedure influences the adsorption and desorption of ZnO surface molecules.



More number of photo-induced oxygen ions are created when the ambient O₂ reacts with the photo-electrons. The photo-carriers that are generated promotes adsorption of O₂ and these highly reactive photo-activated oxygen ions will in turn react with the target gas. The resistance change due to the UV photo-activation was observed to be 50% (36).

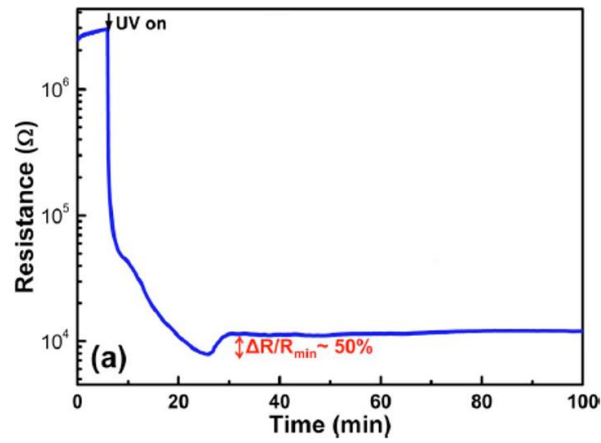


Figure 25. Variation in the resistance after switching on the UV-LED (36).

Yu-Hsuan Ho et al. showed a similar result with enhanced room temperature sensitivity using floccule-like ZnO nanostructures with UV activation throughout the gas sensing process. Octane was used as the testing gas.

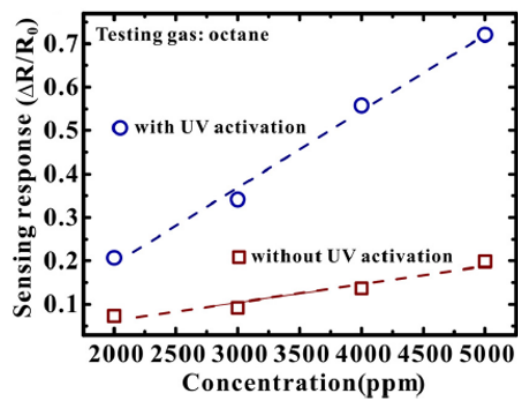


Figure 26. Resistance variation with and without UV irradiation (37).

3.5 Traditional Process of Measuring Sensor Response

Traditional mechanism to determine sensitivity and recovery time of the sensors is by exposing them to the carrier gas and then target gas alternatively. The sensors were exposed to CH₄ for 10 min (adsorbing phase) and under synthetic air for 10 min (desorbing phase) multiple times [Figure 27]. Similar experiment was performed for CH₄ with N₂ as carrier gas [Figure 28]. The recovery time of the sensors is observed to be around 1 to 2 minutes. Reproducibility of the sensors to CH₄ is witnessed. Sensors relative resistance decreases when it is exposed to CH₄, a reducing gas and then rapidly increases when synthetic air or N₂ is introduced into the test chamber.

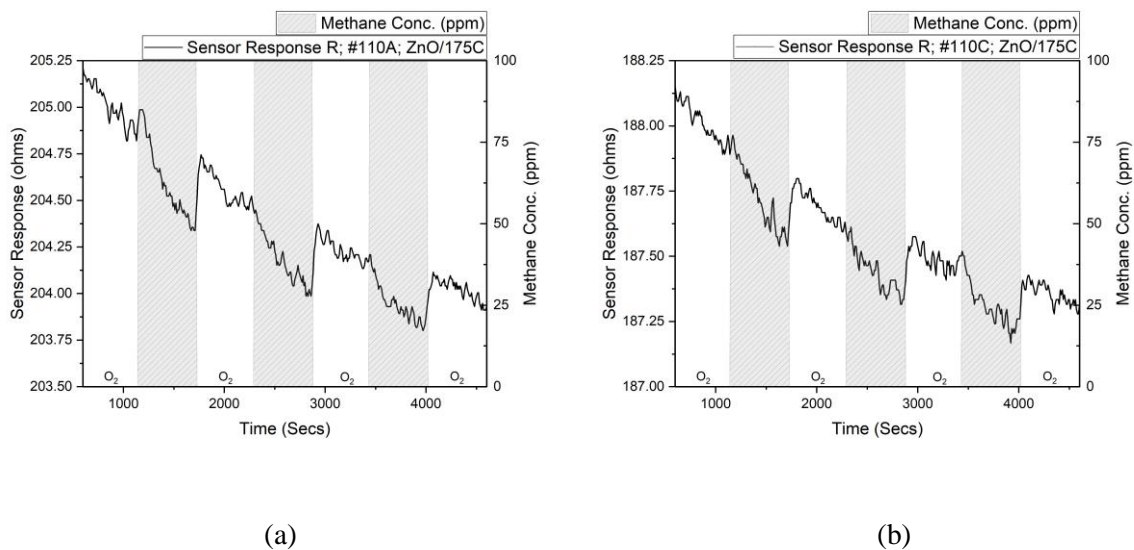


Figure 27. Sensor Response R of ZnO/MWCNT (175⁰C) sensors in ohms under CH₄ and O₂.

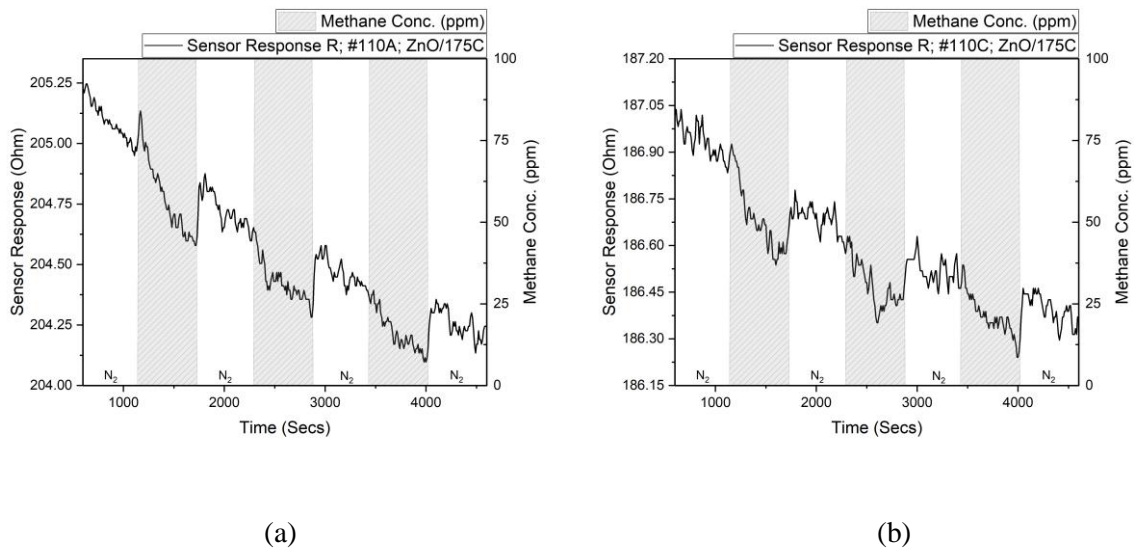


Figure 28. Sensor Response R of ZnO/MWCNT (175⁰C) sensors in ohms under CH₄ and N₂.

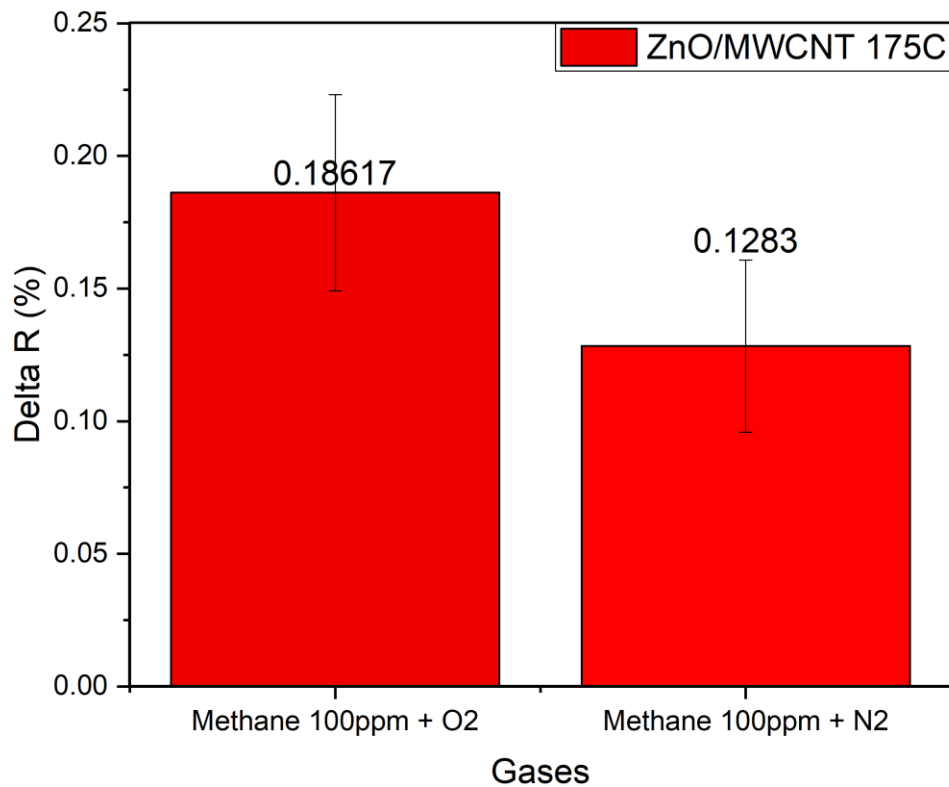


Figure 29. Histogram of relative resistance variation (ΔR) of ZnO/MWCNT (175⁰C) sensors under CH₄ with different carrier gases.

The relative sensitivity of ZnO/MWCNT sensors is calculated using the following equation:

$$\Delta R (\%) = ((R_0 - R_s) / R_0) * 100$$

Where R_0 is the baseline resistance and the R_s is the resistance under target gas.

Stability of the sensors is denoted by standard deviation which is given by,

$$\sigma = \sqrt{\frac{1}{N} \sum_{i=1}^N (x_i - \mu)^2}$$

Where, N denotes number of values, μ is the mean of all the values, x is the individual value, \sum denotes summation of all the values from 1 to N .

The relative sensitivity of ZnO/MWCNT hydrocarbon gas sensors (ALD 175°C) under 100ppm CH₄ with O₂ as carrier gas is 0.186173 ± 0.03699 % [Figure 29].

The relative sensitivity of ZnO/MWCNT hydrocarbon gas sensors (ALD 175°C) under 100ppm CH₄ with N₂ as carrier gas is 0.128299 ± 0.032502 % [Figure 29].

The parameters set used for performing various experiments to analyse UV-degassing effects are given below in Table VI.

TABLE VI
PARAMETERS SET FOR THE UV-DEGASSING STUDY

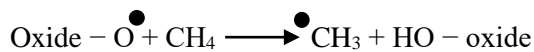
Target Gas	Concentration (ppm)	Carrier Gas	Relative Humidity RH (%)	Storage
Methane	10	20.8% O ₂	2	Room Temperature; Ambient Air
Methane	100	20.8% O ₂	2	
Methane	100	N ₂	2	
Benzene	50	N ₂	2	
Toluene	10	N ₂	2	

3.6 UV-degassing Mechanism

ZnO/MWCNT is continuously exposed to CH₄ gas under ambient light and room temperature with relative humidity (RH) of 2%. After a warm up period of 60 minutes under the carrier gas i.e. synthetic air (20.8% O₂, 79.2% N₂) or 100% N₂, the sensors are exposed to the target gas. Resistance change i.e. resistance versus time is measured for the entire period. During the continuous exposure to CH₄ gas, the sensor is periodically exposed to UV-irradiation every 20 minutes for a total exposure time of 12 seconds each time. It is known that ZnO has a band gap of 3.2eV and a light with energy equal to or higher than its band gap needs to be used for irradiation. Hence, UV light of wavelength 365nm was chosen for the study to irradiate the ZnO surface.

Mechanism:

The below chemical equations describes the mechanism of reformation of ZnO material on the MWCNT when UV light is illuminated. The broader view of the mechanism is given as (38),



When ZnO is illuminated under UV, the surface electron and hole is generated.



The generated electron and hole will attract the hydrogen atom from CH₄ molecule and pairs up. Upon UV illumination, the oxygen molecules are adsorbed on the surface of ZnO nanoparticles and extract electrons from the conduction band forming oxygen species as shown in (2).



Further oxidation of the methyl radicals are as given below.



After the ZnOH gets oxidized to ZnO, the reaction repeats from (2) forming a cyclic loop of the reactions. The Zinc radical in turn reacts with CH₄ to form methyl radical (\bullet CH₃). The methyl radical react with oxygen ions, which subsequently results in the re-formation of ZnO. Thus, the restoring the electrical and photocatalytic properties of the ZnO.

The schematic illustration of the photo-catalytic reaction of methane is given in Figure 30, which clearly shows a cyclic reaction. Exposure of the sensors to the target gas over a period of time will gradually degenerate its ability to sense i.e. sensitivity of the sensors towards the target gas weakens. As shown below, methane oxidation is a two-step process. In the first step, a series of reactions (1) to (5) takes place where CH₄ reacts with O₂ to produce water and formaldehyde. With UV illumination, further oxidation of the formaldehyde occurs to generate CO₂ and H₂O; thus accommodating more surface area on the ZnO surface for target gas molecules reactions (39). As a result, using UV illumination resolves the issue w.r.t long term stability of the sensors.

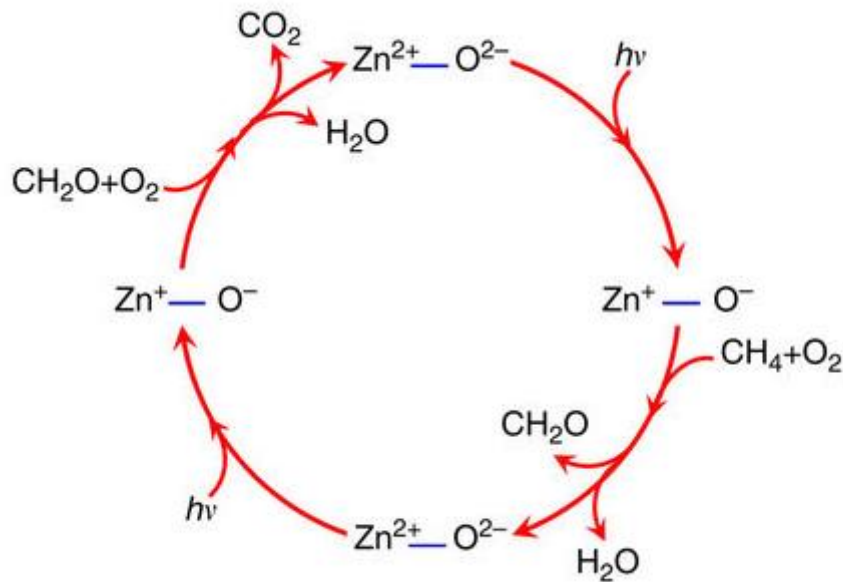


Figure 30. Schematic illustration of the photo-catalytic reaction process of CH₄ (39).

MWCNT extract the electrons to prevent the recombination of electrons with the holes on the surface of ZnO. Once the CH₄ molecules are adsorbed on the ZnO surface, reactions (2) to (5) takes place which will eventually free the electrons on ZnO surface. This results in the increase in conductivity and decrease in the resistance. Similar behaviour has been observed with benzene and toluene gases as well.

3.7 Experimental Results

Figures 31 - 33 shows the resistance vs. time graphical representation and analysis of UV-degassing effect for Methane (10 ppm), Benzene (50 ppm) and Toluene (10 ppm) gases, respectively.

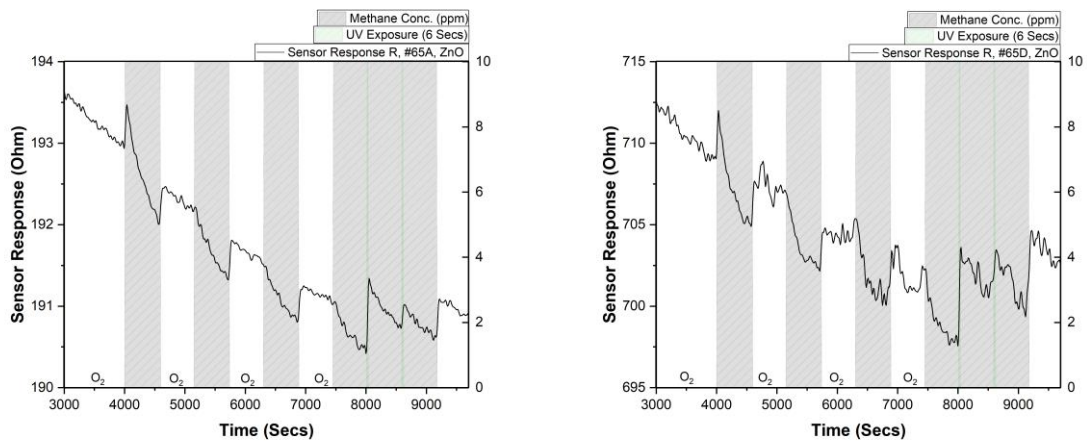


Figure 31. Sensor Response R and UV-degassing effect of ZnO/MWCNT (175⁰C) sensors; Methane and O₂ as carrier gas.

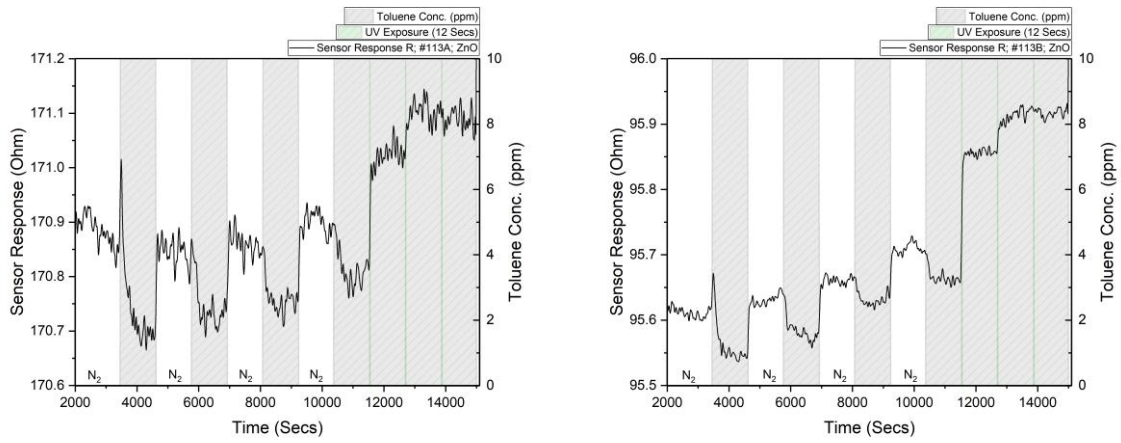


Figure 32. Sensor Response R of ZnO/MWCNT (175⁰C) sensors; Toluene and N₂ as carrier gas.

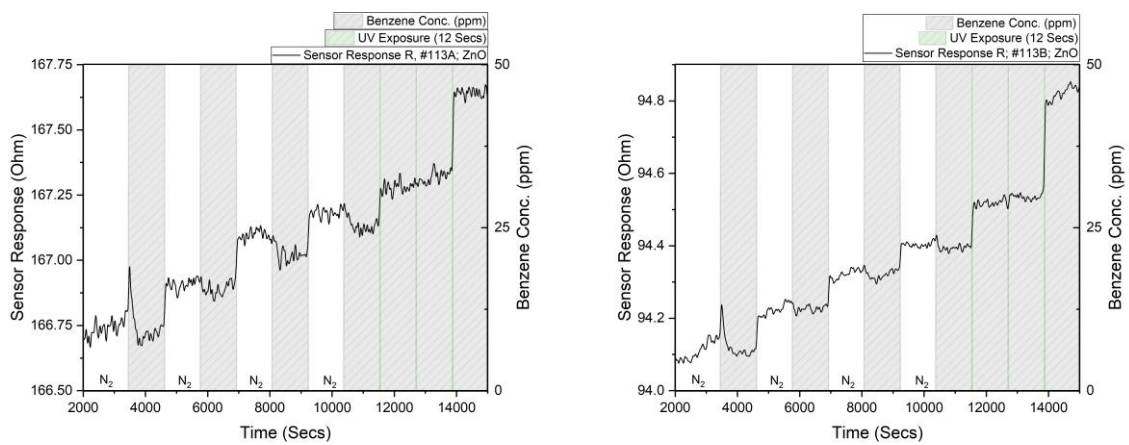


Figure 33. Sensor Response R of ZnO/MWCNT (175⁰C) sensors; Benzene and N₂ as carrier gas.

Figures 34 - 35 shows the UV-degassing effect for Methane (100 ppm) with synthetic air and N₂ as carrier gases respectively.

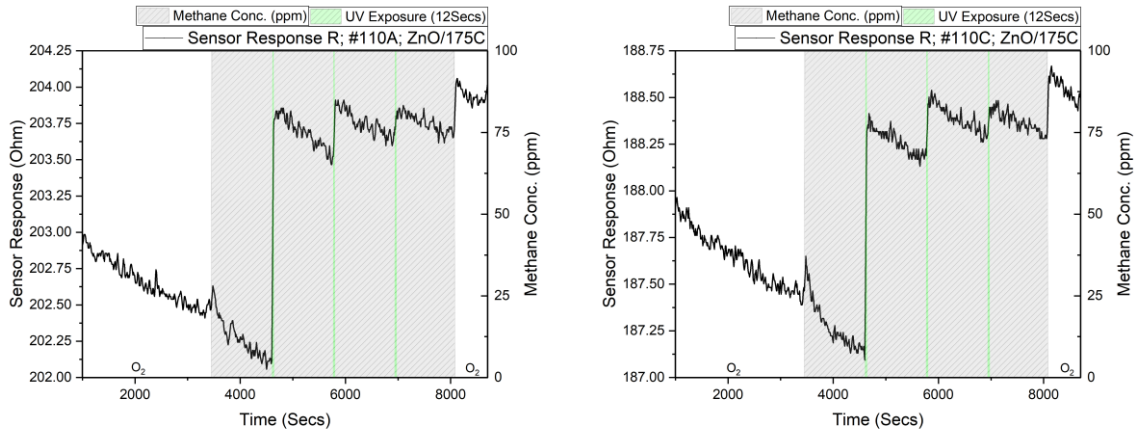


Figure 34. UV-degassing effect of ZnO/MWCNT (175⁰C) sensors; Methane and O₂ as carrier gas.

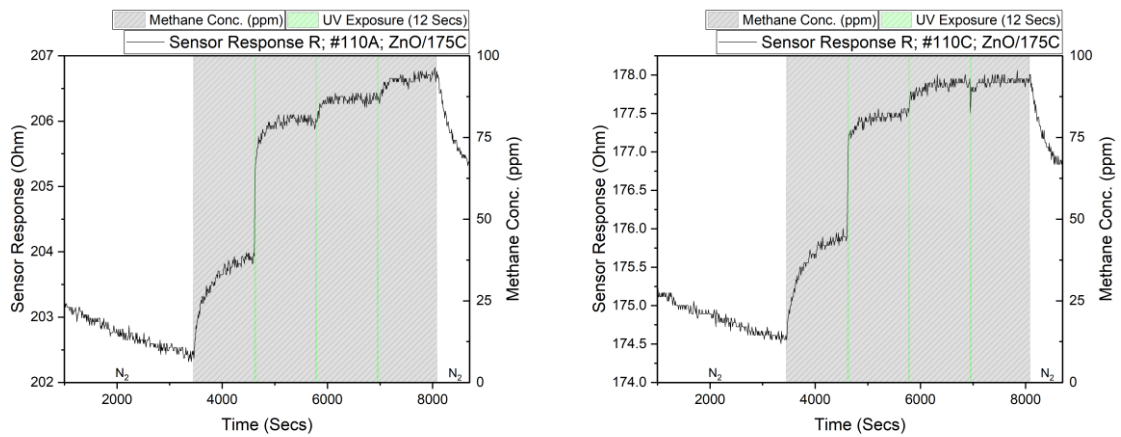


Figure 35. UV-degassing effect of ZnO/MWCNT (175⁰C) sensors; Methane and N₂ as carrier gas.

The results from Figures 31, 32 and 33 clearly shows that the UV degassing effect is observed only when the sensors are exposed to Methane gas with synthetic air as carrier gas and not when exposed to VOCs. This is due to lack of oxygen molecules required for the UV degassing mechanism, since N₂ is used as a carrier gas for experiments with VOCs. The sensors do not achieve baseline (R₀), though a change in the resistance (sensitivity) is observed.

It is observed that the sensors resistance quickly decrease when exposed to CH₄ and then quickly increases within 10 seconds when exposed to UV light, restoring its initial electrical and photo-catalytic properties by achieving baseline, R₀. This denotes the re-formation of the ZnO on MWCNT material, thus re-establishing its chemical reactivity towards CH₄. As a result, the sensor properties are refreshed and thus, solves the problem of long range signal drift over a period of exposure to target gas.

Figure 31 is the graphical representation of resistance vs. time when exposed under Methane with Synthetic air as the carrier gas ($0.436966 \pm 0.049759043\%$). Figure 32 and 33 shows the graphical representation of the sensor's resistance change when exposed under Benzene and Toluene ($0.025549 \pm 0.011238 \%$; $0.05539 \pm 0.028482 \%$), respectively, nitrogen being the carrier gas.

In the initial phase, the sensors are exposed in alternate cycles to CH₄ and Synthetic air to determine sensitivity of the sensors under the exposure of the target gas. In the next phase, the sensors are continuously exposed to the target gas and UV light of 365nm wavelength is illuminated multiple times for 6 seconds (for Methane) and 12 seconds (for VOCs) at an interval of 20 minutes.

In order to confirm the oxygen dependency of the UV-degassing mechanism, an experiment was conducted with Methane as the target gas and N₂ as the carrier gas. This experiment was performed to compare the behaviour of the sensors under CH₄ with N₂ to that of behaviour under VOCs with N₂ as carrier gases, upon UV illumination. Figures 34 and 35 demonstrates the sensor responses under two different carrier gases O₂ and N₂, respectively. The carrier gas was introduced into the test chamber initially for 60 minutes to purge the humidity within the chamber. Thus, these molecules got deposited on the sensors surface. Then, the sensors were continuously exposed to the target gas (CH₄). UV light was illuminated for 12 seconds multiple times at an interval of 20 minutes time duration.

It is observed that the sensor responses under exposure to VOCs and CH₄ with N₂ are similar upon UV illumination, thus proving the oxygen dependency for UV-degassing mechanism. UV-degassing effect is not observed when N₂ is used as the carrier gas.

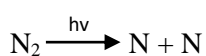
3.8 Discussion

The removal of the surface contaminant is observed upon UV illumination when exposed to VOCs [Figure 32, 33, 35], whereas the sensors response do not achieve baseline. The increase in the number of electrons on the surface due to photo-activation boosts the oxidization process of the surface organic contaminant as well. As a result, the surface of the sensing layer gets cleaned thereby enhancing gas adsorption.

As described above, more photo-activated oxygen ions are generated upon UV illumination, which will eventually react with the target gas. There might be a possibility that lack of more oxygen ions on the surface in order to react with the target gas might have resulted in the failure of UV degassing effect using VOCs.

Li-Ko Yeh et.al demonstrated photo-activation for Toluene sensing at room temperature on Coral-like ZnO nanostructure. Ambient air containing 20.95% oxygen was considered as the carrier gas. Higher the target gas concentration, more is the sensitivity observed. This is due to the availability of more toluene molecules to react with the oxygen ions on the ZnO surface (40). From these observations and results demonstrated, it can be inferred that UV Degassing mechanism is Oxygen dependent.

It has also been observed that the Nitrogen molecule reacts with the Methane and VOCs as the target gases. A significant variation in the sensor's resistance (ΔR) is observed when using N₂ as carrier gas. Hence, another possibility for the failure of UV-degassing effects using N₂ could be due to unable to photo-dissociate of N₂ upon UV illumination with 365nm wavelength. O₂ photo-dissociates to two single oxygen atoms when it comes under the influence of UV light. Similarly, N₂ photo-dissociates to two single nitrogen atoms.



The triple bond of Nitrogen molecule is much stronger than the double bond in the Oxygen molecule. Thus, it requires a very high bond dissociation energy of 9.79 eV/bond (945 kJ/mol) to photo-dissociate the

Nitrogen molecule. Nitrogen dissociates only in the vacuum ultraviolet exposure which has a wavelength of 10 to 200 nm. (41, 42)

The chemistry behind the reaction of N_2 under UV exposure needs to be further explored to get a better picture of the chemical reaction that is taking place. Using extreme UV for degassing process was beyond the scope of this project.

CHAPTER 4

REJUVENATION OF AGED SENSORS

4.1 Experimental Methodology

Over a period of time, due to constant exposure to the target gases, the sensor's sensitivity towards the target gases gradually deteriorates. The humidity in the ambient room conditions also play a major role in progressive aging of the sensors. Accumulation of the water molecules on the surface of the ZnO/MWCNT film stimulates aging process, since it eventually reduces the surface area for sensing the target gas. Electrons are not created on the metal oxide surface as a result of water adsorption. Adsorbed water molecules react with the oxygen ions on the surface to form less reactive hydroxyl groups, potentially obstructing the gas sensing reaction (43). They lower the baseline resistance of the gas sensors and thus, decreases the sensor's sensitivity towards the target gas. A drift in the response generally occurs due to aging, which is a slow process.

High surface area on the sensing film is necessary to allow for the effective reactions to take place between the gas sensing material and target gases. As a result, removal of the surface contaminant is another step necessary to rejuvenate the aged sensors.

The methodology to rejuvenate the sensors is tailored in such a way that it handles each of the above mentioned factors that bases the aging process of the sensors. Any contaminants were accumulated on the sensor surface over a period of time is removed by illuminating UV on the surface of the sensors for 24 seconds.

Next, in order to counter the humidity effect, the sensors are baked at 80°C for 1 to 2 hours on a hot plate. Desorption of the water molecules from the surface occurs under the application of heat.

The sensors are then stored in a closed chamber for few hours to let the sensors cool down and stabilize.

The steps implemented to rejuvenate aged sensors whose sensitivity had degraded is summarized below.

Step 1: Performed experiment to determine the initial sensitivity of the sensor towards target gas.

Step 2: UV light of wavelength 365 nm is illuminated for a duration of 24 seconds.

Step 3: Sensors are baked at 80°C for 1 to 2 hours.

Step 4: Stored under ambient air and room temperature within a closed chamber for 8 to 10 hours.

The summary of the parameters set considered for rejuvenation process are given in Table VII.

TABLE VII
PARAMETERS SET FOR REJUVENATION PROCESS

Parameters	Values
UV Light Wavelength	365 nm
Duration of UV Exposure	24 Seconds
Baking Temperature using Hot Plate	80°C
Duration of Baking	1 – 2 Hours
Storage Conditions	Ambient Air, Room Temperature (In a Closed Chamber)
Storage Duration	8 – 10 Hours

As a part of the preliminary analysis of the sensor's behaviour, after each step mentioned above, an experiment was performed to check for any improvement in the sensor's response R. The sensors are exposed to alternate cycles of CH₄ and Synthetic air (20.8% O₂, 79.2% N₂) for 20 minutes each. The responses are monitored for 3 cycles.

4.2 Experimental Results and Observations

Figures 36 – 39 shows the sensor response of the aged sensors after each step of the rejuvenation process.

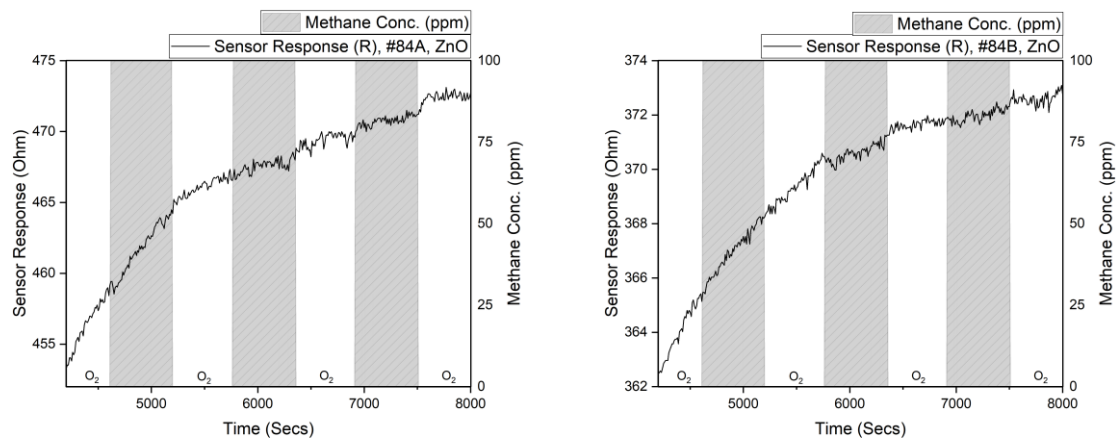


Figure 36. ZnO/MWCNT (175⁰C) aged sensors initial response.

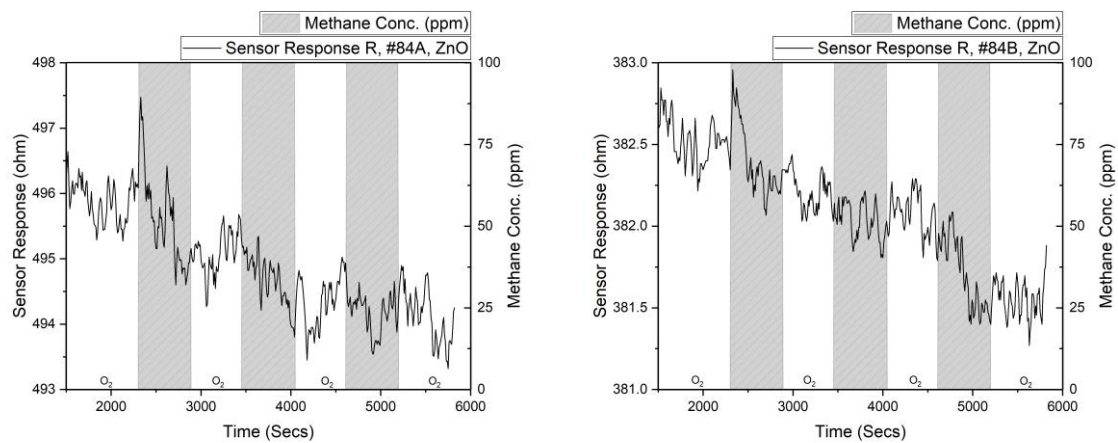


Figure 37. ZnO/MWCNT (175⁰C) aged sensors response after exposure to 24 seconds of UV light.

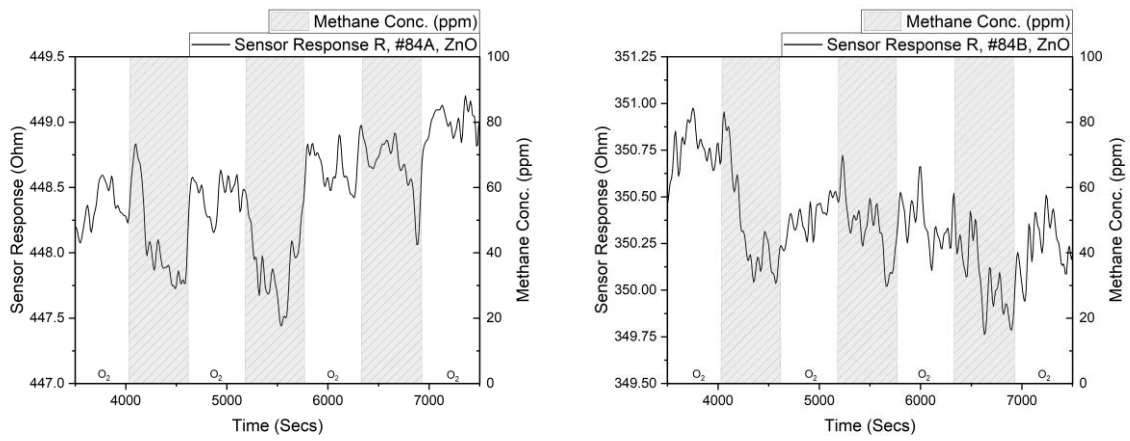


Figure 38. ZnO/MWCNT (175⁰C) aged sensors response after baking at 80⁰C and then storing.

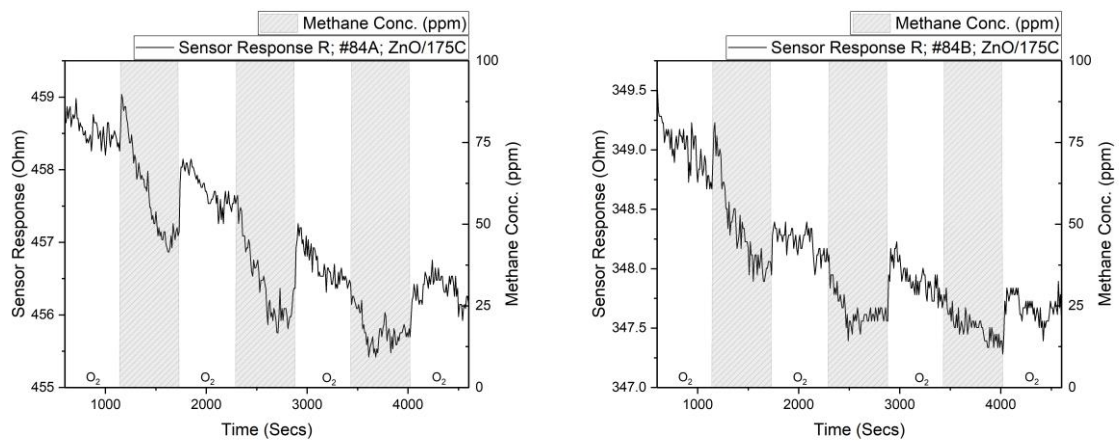


Figure 39. ZnO/MWCNT (175⁰C) aged sensors response after rejuvenation process.

Initially, no response was observed towards the target gas by the sensors 84A and 84B which determined that they are aged [Figure 36]. After exposing to UV light for 24 seconds, the response observed is highly insignificant due to profuse noise in the response [Figure 37]. After the next step of baking the sensors at

80°C for 1 to 2 hours and then storing in a closed chamber, the sensors response significantly improved [Figure 38].

A confirmatory test was performed on the same sensors by repeating the steps, however, the experiment to analyse the improvement in the sensitivity of the sensors was conducted after all the steps (from 2 to 4) of the rejuvenation process was performed. The sensors have shown a very good sensitivity towards Methane gas. Sensor 1 (#84A) demonstrated a relative sensitivity of 0.176496 ± 0.063826 %, whereas the sensor 2 (#84B) demonstrated 0.242703 ± 0.083933 % [Figure 39].

4.3 Discussion

Gas sensing process is strongly related to surface reactions of the sensing material. Aging leads to drift in the sensor's response. Aging is a natural phenomenon for sensors since the sensing film is under constant exposure to the surrounding environment and the target gas. Surface contaminants were accumulated over the sensing surface over a period of time. It is very essential to rejuvenate the aged sensors to avoid their frequent replacement, which could incur additional cost. Aging hampers the accuracy in the measurements, which could lead to serious catastrophes.

The methodology that was implemented for the study has given good results with a significant improvement in the sensor's sensitivity towards Methane. There is an enormous scope for further analysis by tuning each parameters and by repeating the steps multiple times. The relative humidity in the ambient air also needs to be monitored during analysis.

CHAPTER 5

CONCLUSION AND FUTURE WORK

5.1 Conclusion

Hetero-structured gas sensors based on Multi-walled Carbon nanotubes functionalized with Zinc Oxide nanoparticles were used for this study. The study mainly focusses on the detection of hydrocarbon gases. Despite their good sensitivity, chemiresistive sensors based on MOX suffers from low stability and long range signal drift over time, which leads to the necessity to re-calibrate or replace the sensors frequently. UV-degassing has proven to be a possible mechanism that could solve the problem by re-establishing the electrical and photocatalytic properties of the ZnO. From the analysis it was determined that the UV-degassing mechanism is Oxygen dependent for the parameters set that were considered. The possibility of degassing using Nitrogen as the carrier gas needs to be further explored.

A method to rejuvenate aged sensors was developed and implemented considering humidity and surface contaminants as the main factors influencing the aging of the sensors. A significant improvement in the sensors response was observed, thus demonstrating it as an effective approach to rejuvenating aged sensors.

5.2 Future Work

In order to explore the UV-degassing effects under the Nitrogen gas, implementing the mechanism under extreme UV of high intensities could be next possible work.

Tweaking various parameters from the parameters set used for the rejuvenation experiment may possibly provide varied results. Hence, it is necessary to analyse the effects of each parameter in rejuvenating the aged sensors.

UV-degassing effects could be studied on MOX/MWCNT sensors with various photo-catalysts like TiO₂, SiO₂, etc. and the results can be compared with that of ZnO/MWNT sensor.

CITED LITERATURE

1. Monitoring of Hydrocarbons and Organics. Retrieved from: <http://hub.globalccsinstitute.com/node/102726>
2. Greenhouse Gas Emissions. Retrieved from: <https://www.epa.gov/ghgemissions/understanding-global-warming-potentials>
3. Taguchi, N.: GAS DETECTING DEVICE. 3,695,348, 1972
4. Joo, S. and Brown, R.B: Chemical Sensors with Integrated Electronics. *Chem. Rev.*, 108 (2), pp 638–651, 2008
5. Alenezi, M.R., Alshammari, A.S., Jayawardena, K.D.G.I., Beliatis, M.J., Henley, S.J., and Silva, S.R.P.: Role of the Exposed Polar Facets in the Performance of Thermally and UV Activated ZnO Nanostructured Gas Sensors. *The Journal of Physical Chemistry C* 117 (34), 17850-17858, 2013
6. Fine, G.F., Cavanagh, N.M., Afonja, A., and Binions, R.: Metal Oxide Semi-Conductor Gas Sensors in Environmental Monitoring. *Sensors*, 10(6), 5469-5502, 2010
7. Ogawa, H., Nishikawa, M., and Abe, A.: Hall measurement studies and an electrical conduction model of tin oxide ultrafine particle films. *J. Appl. Phys.*, 53, 4448–4455, 1982
8. Parkin, I.P., Binions, R., Piccirillo, C., Blackman, C.S., and Manning, T.D.: Thermo-chromic Coatings for Intelligent Architectural Glazing. *Journal of Nano Research*, Vol. 2, pp. 1-20, 2008
9. Neri, G.: First Fifty Years of Chemoresistive Gas Sensors. *Chemosensors*, 3, 1-20, 2015
10. Binions, R.; Carmalt, C.J.; Parkin, I.P.: Aerosol-assisted chemical vapour deposition of sodium fluoride thin films. *Thin Solid Films*, 469–470, 416–419, 2004
11. Aswal, D.K., Gupta, S.K.: Science and Technology of Chemiresistor Gas Sensors, Pages 4-49
12. Yamazoe, N.: Toward innovations of gas sensor technology. *Sensors Actuators, B Chem*, Volume 108, Pages 2-14, 2005
13. Yamazoe, N., Sakai, G., and Shimanoe, K.: Oxide semiconductor gas sensors. *Catalysis Surveys from Asia*, Volume 7, Number 1, Page 63, 2003
14. Barsan, N., and Weimar, U.: Conduction model of metal oxide gas sensors. *Journal of Electroceramics*, Volume 7, Number 3, Page 143, 2001
15. Sahm, T., Gurlo, A., Barsan, N., Weimar, U., and Madler, L.: Fundamental studies on SnO₂ by means of simultaneous work function change and conduction measurements. *Thin Solid Films*, Volume 490, Issue 1, Pages 43-47, 2005
16. Liu, L., Ye, X., Wu, K., Han, R., Zhou, Z., and Cui, T.: Humidity Sensitivity of Multi-Walled Carbon Nanotube Networks Deposited by Dielectrophoresis. *Sensors*, 9(3), 1714-172, 2009
17. Korotcenkov, G.: Handbook of Gas Sensor Materials, 2014
18. Dresselhaus, M.S., Dresselhaus, G, and Eklund, P.C.: Science of Fullerenes and Carbon Nanotubes, 1996.

CITED LITERATURE (continued)

19. Scientists Delve Deeper into Carbon Nanotubes. Retrieved from: <http://physicsworld.com/cws/article/news/2013/feb/19/scientists-delve-deeper-into-carbon-nanotubes>
20. Ajayan, I.M., Schadler, L.S., and Braun, P.V.: Nanocomposite Science and Technology, 2004
21. Sarkar, S., Bekyarova, E., Niyogi, S., and Haddon, R.C.: Diels–Alder Chemistry of Graphite and Graphene: Graphene as Diene and Dienophile. *J. Am. Chem. Soc.*, 133 (10), Pages 3324–3327, 2011
22. Study Reveals Organic Semiconductors’ Overwhelming Thermoelectric Efficiency. Retrieved from: <http://www.machinedesign.com/materials/study-reveals-organic-semiconductors-overwhelming-thermoelectric-efficiency>
23. Tang, R., Shi, Y., Hou, Z., and Wei, L.: Carbon Nanotube-Based Chemiresistive Sensors. *Sensors* (Basel, Switzerland) 17(4): 882, 2017
24. Zhang, W.D., and Zhang, W.H.: Carbon Nanotubes as Active Components for Gas Sensors. *Journal of Sensors*, Article ID 160698, 16 pages, 2009
25. Jeon, I.Y., Chang, D.W., Kumar, N.A., and Baek, J.B.: Functionalization of Carbon Nanotubes – Polymer Nanocomposites. Retrieved from: <https://mts.intechopen.com/books/carbon-nanotubes-polymer-nanocomposites/functionalization-of-carbon-nanotubes>, 2011
26. Liu, X., Cheng, S., Liu, H., Hu, S., Zhang, D., and Ning, H.: A Survey on Gas Sensing Technology. *Sensors* (Basel), 12(7): 9635–9665, 2012
27. Tech Brief: A Look at Atomic Layer Deposition (ALD). Retrieved from: <https://blog.lamresearch.com/tech-brief-a-look-at-atomic-layer-deposition-ald/>
28. Humayun, M., Divan. R., Stan, L., Gupta, A., Rosenmann, D., Gundel, L., Solomon, P., and Paprotny, I.: ZnO Functionalization of Multi-walled Carbon Nanotubes for Methane Sensing at Single Parts per Million Concentration Levels. *Journal of Vacuum Science & Technology B*. American Institute of Physics, NY, 33(6):1-7, 2015
29. Chen, H., Liu, Y., Xie, C., Wu, J., Zeng, D., and Liao, Y.: A comparative study on UV light activated porous TiO₂ and ZnO film sensors for gas sensing at room temperature. *Ceramics International*, Volume 38, Issue 1, Pages 503-509, 2012
30. Comini, E., Cristalli, A., Faglia, G., and Sberveglieri, G.: Light enhanced gas sensing properties of indium oxide and tin dioxide sensors. *Sensors and Actuators B: Chemical*, Volume 65, Pages 260–263, 2000.
31. What is Photocatalyst? Retrieved from: <http://www.greenearthnanoscience.com/what-is-photocatalyst.php>
32. Wang, C., Yin, L., Zhang, L., Xiang, D., and Gao, R.: Metal oxide gas sensors: sensitivity and influencing factors. *Sensors* (Basel), Volume10, 2088–2106, 2010
33. Wisz, G., Virt, I., Sagan, P., Potera, P., and Yavorskyi, R.: Structural, Optical and Electrical Properties of Zinc Oxide Layers Produced by Pulsed Laser Deposition Method. *Nanoscale Research Letters*, Volume 12, Page 253, 2017

CITED LITERATURE (continued)

34. ZnO bandgap engineering. Retrieved from: http://maeresearch.ucsd.edu/mckittrick/index_files/Page945.html
35. Hariharan, C.: Photocatalytic degradation of organic contaminants in water by ZnO nanoparticles. *Applied Catalysis A: General*, Volume 304, Pages 55-61, 2006
36. Fan, S.W., Srivastava, A.K., and Dravid, V.P.: UV-activated room-temperature gas sensing mechanism of polycrystalline ZnO. *Applied Physics Letters* 95, 142106, 2009
37. Ho, Y.H., Huang, W.S., Chang, H.C., Wei, P.K., Sheen, H.J., and Tian, W.C.: Ultraviolet-enhanced room-temperature gas sensing by using floccule-like zinc oxide Nanostructures. *Applied Physics Letters* 106, 183103, 2015
38. Sainato, M., Divan, R., Stan, L., Liu, Y., Sahagun, A., Xiang, J., and Paprotny, I.: Multi-Walled Carbon Nanotube (MWCNT) Metal Oxide Nanocrystal (MOX NC) ZnO Sensors for Selective Sensing of VOCs and CH₄. *Unpublished*
39. Chen, X., Li, Y., Pan, X., Cortie, D., Huang, X., and Yi, Z.: Photocatalytic oxidation of methane over silver decorated zinc oxide nanocatalysts. *Nature Communications*, Volume 7, Article number: 12273, 2016
40. Yeh, L.K., Luo, J.C., Chen, M.C., Wu, C.H., Chen, J.Z., Cheng, I.C., Hsu, C.C., and Tian, W.C.: A Photoactivated Gas Detector for Toluene Sensing at Room Temperature Based on New Coral-Like ZnO Nanostructure Arrays. *Sensors*, Volume 16(11), 1820, 2016
41. Chakraborty, S., Jackson, T.L., Rude, B., Ahmed, M., and Thiemens, M.H.: Nitrogen isotopic fractionations in the low temperature (80 K) vacuum ultraviolet photodissociation of N₂. *The Journal of Chemical Physics*, Volume 145, Issue 11, 2016
42. Bond-dissociation energy. Retrieved from: https://en.wikipedia.org/wiki/Bond-dissociation_energy
43. Traversa, E.: Ceramic Sensors for Humidity Detection: The State-of-the-art and Future Developments. *Sensors and Actuators B: Chemical*, Volume 23, Issues 2–3, Pages 135-156, 1995

VITA

- NAME:** Mrudula Manjunath
- EDUCATION:** B.E., Electronics and Communication Engineering, B N M Institute of Technology (Affiliated to VTU), Bengaluru, India, 2011
- Project: Design, Analysis & Implementation of DSP Based Low Power and Computationally Efficient 1D-IDCT Using Chen's Algorithm in JPEG CODEC
- M.S., Electrical and Computer Engineering, University of Illinois at Chicago, IL, USA, 2018
- Thesis: ZnO/MWCNT Sensors: Rejuvenation and Analysis of UV-Degassing Effects for Hydrocarbon Gases
 - Adviser: Prof. Igor Paprotny
- EXPERIENCE:** Micro-mechatronic Systems Laboratory, University of Illinois at Chicago, IL, USA
- Graduate Student Researcher, May 2017 – May 2018
 - Adviser: Prof. Igor Paprotny
 - Focus: Carbon Nanotubes based gas sensors – Rejuvenation and degassing, soldering
- Colca, LLC, Chicago, Illinois, USA
- Embedded Systems Development Intern, January 2018 – March 2018
 - Work: Hardware development, PCB design, Hardware integration with micro-controller, C programming for microcontroller, testing and debugging – hardware and firmware
- Mphasis Wyde, Bengaluru, India
- Delivery Software Engineer, July 2012 – June 2016
 - Work: Software development for the Insurance product - Development, enhancements and bug fixing, scheduled over agile methodology
 - Led the team of three young developers
 - Programming Languages: GOLD, C, SQL, OOPs; Environments: eWAM v6.0, Wynsure v5.0
- National Institute of Technology, Karnataka, India
- Project Associate, February 2012 – July 2012
 - Work: Coal India Limited sponsored R&D project on 'Modelling of airborne dust in opencast coal mines' - Assessed the performance of Explosive/Blast result based on the Explosive Energy Utilization
- AWARDS:** Mphasis Annual Award for the best "Service Delivery Excellence Team", 2014.
- PROFESSIONAL AFFILIATION:** Society of Women Engineers, Chicago Chapter, IL, USA, 2016 – 2018